Experimental Eye Research 247 (2024) 110062

Contents lists available at ScienceDirect

Experimental Eye Research

journal homepage: www.elsevier.com/locate/yexer

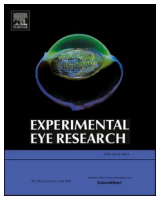

Research article

VEGF-A_{165}a and angiopoietin-2 differently affect the barrier formed by retinal endothelial cells

Heidrun L. Deissler [a,*], Matus Rehak [a,b,1], Lyubomyr Lytvynchuk [a,1]

[a] Department of Ophthalmology, Justus Liebig University Giessen, Giessen, Germany
[b] Department of Ophthalmology, Medical University of Innsbruck, Innsbruck, Austria

ARTICLE INFO

Keywords:
Retinal endothelial cells
VEGF-A
Angiopoietin-2
Bevacizumab
Faricimab
Tivozanib
Barrier stability
Tight junction
Adherens junction
Internalization

ABSTRACT

Exposure to VEGF-A_{165}a over several days leads to a persistent dysfunction of the very tight barrier formed by immortalized endothelial cells of the bovine retina (iBREC). Elevated permeability of the barrier is indicated by low cell index values determined by electric cell-substrate impedance measurements, by lower amounts of claudin-1, and by disruption of the homogenous and continuous staining of vascular endothelial cadherin at the plasma membrane. Because of findings that suggest modulation of VEGF-A's detrimental effects on the inner blood-retina barrier by the angiogenic growth factor angiopoietin-2, we investigated in more detail *in vitro* whether this growth factor indeed changes the stability of the barrier formed by retinal endothelial cells or modulates effects of VEGF-A. In view of the clinical relevance of anti-VEGF therapy, we also studied whether blocking VEGF-A-driven signaling is sufficient to prevent barrier dysfunction induced by a combination of both growth factors. Although angiopoietin-2 stimulated proliferation of iBREC, the formed barrier was not weakened at a concentration of 3 nM: Cell index values remained high and expression or subcellular localization of claudin-1 and vascular endothelial cadherin, respectively, were not affected. Angiopoietin-2 enhanced the changes induced by VEGF-A_{165}a and this was more pronounced at lower concentrations of VEGF-A_{165}a. Specific inhibition of the VEGF receptors with tivozanib as well as interfering with binding of VEGF-A to its receptors with bevacizumab prevented the detrimental effects of the growth factors; dual binding of angiopoietin-2 and VEGF-A by faricimab was marginally more efficient. Uptake of extracellular angiopoietin-2 by iBREC can be efficiently prevented by addition of faricimab which is also internalized by the cells. Exposure of the cells to faricimab over several days stabilized their barrier, confirming that inhibition of VEGF-A signaling is not harmful to this cell type. Taken together, our results confirm the dominant role of VEGF-A_{165}a in processes resulting in increased permeability of retinal endothelial cells in which angiopoietin-2 might play a minor modulating role.

1. Introduction

Macular edema secondary to diabetic retinopathy (DR) and retinal vein occlusion are diseases of high clinical and socio-economic relevance (Campochiaro, 2000, 2013). Their pathogeneses are closely associated with the deregulated expression of growth factors and cytokines, reflected by their elevated concentrations in the vitreous of affected patients (Aiello et al., 1994; Boulton et al., 1997; Watanabe et al., 2005; Kinnunen et al., 2009; Klaassen et al., 2017, 2022). The dominant role of vascular endothelial growth factor-A (VEGF-A) in the development of macular edema is due to the ability of its splice variant VEGF-A_{165}a to persistently enhance the permeability of retinal endothelial cells (REC) (Antonetti et al., 1999; Deissler et al., 2011; Qaum et al., 2001). VEGF-A_{165}a, but not its splice variant VEGF-A_{165}b differing in six C-terminal amino acids, induces dysfunction of the barrier formed by REC by binding to and thereby activating the VEGF receptor 2 (VEGFR2) (Eichmann and Simons, 2012; Smith et al., 2015; Bates et al., 2018; Deissler et al., 2017, 2020a). Acknowledging the dominant role of VEGF-A_{165}a, it still is a plausible assumption that its action of is modulated by other growth factors or cytokines present in the vitreous of DR patients. Among these, the angiogenic growth factor angiopoietin-2 (ANG2) has been identified as a particularly interesting secondary target that is found strongly upregulated in vitreous samples

* Corresponding author. Department of Ophthalmology, Justus Liebig University Giessen, Friedrichstrasse 18, 35392, Giessen, Germany.
E-mail addresses: heidrun.deissler@augen.med.uni-giessen.de (H.L. Deissler), matus.rehak@i-med.ac.at, matus.rehak@tirol-kliniken.at (M. Rehak), lyubomyr.lytvynchuk@augen.med.uni-giessen.de (L. Lytvynchuk).
[1] Both authors contributed equally.

https://doi.org/10.1016/j.exer.2024.110062
Received 9 April 2024; Received in revised form 25 July 2024; Accepted 23 August 2024
Available online 24 August 2024

Abbreviations

AJ	adherens junction
ANG1/2	angiopoietin-1/2
CI	cell index
DR	diabetic retinopathy
EC	endothelial cells
ECGM	endothelial cell growth medium
FBS	fetal bovine serum
FcRn	neonatal Fc receptor/transporter
hEGF	human epidermal growth factor
HRP	horseradish peroxidase
HuREC	human retinal endothelial cells
iBREC	immortalized bovine retinal endothelial cells
IF	immunofluorescence
PBS	phosphate-buffered saline
PBSd	PBS without Ca^{2+} and without Mg^{2+} ions
REC	retinal endothelial cells
RP	retinal pericytes
TEER	transendothelial electrical resistance
TJ	tight junction
SD	standard deviation
VEcadherin	vascular endothelial cadherin
VEGF-A	vascular endothelial growth factor-A
VEGFR	vascular endothelial growth factor receptor
WB	Western blot analyses

of many DR patients (Watanabe et al., 2005; Kinnunen et al., 2009; Klaassen et al., 2022; Regula et al., 2016; Khan et al., 2020; Nguyen et al., 2020). ANG2 is predominantly produced by endothelial cells (EC) of macro- and microvascular beds including REC and stored in EC-specific Weibel-Palade bodies from which it can be released shortly after stimulation (Fiedler et al., 2004; Pergolizzi et al., 2018). If VEGF-A can indeed induce expression or secretion of ANG2 by (retinal) EC is still under debate, higher expression of the corresponding mRNA after extended treatment of human REC (HuREC) with VEGF-A_{165} has been shown (Fiedler et al., 2004; Regula et al., 2016; Pergolizzi et al., 2018; McCann et al., 2023). In the regulation of angiogenesis and pathological processes affecting stability of the vasculature VEGF-A and ANG2 can act in concert, but through activation of independent signaling pathways. ANG2 exerts its effects by binding to the receptor tyrosine kinase Tie2, at which it is a competing antagonist of angiopoietin-1 (ANG1), the ligand that can induce Tie2 phosphorylation (Maisonpierre et al., 1997; Saharinen et al., 2010; Nguyen et al., 2020).

Because previous investigations addressing the question whether ANG2 by itself might impair the barrier formed by REC or modulate the barrier-disturbing effect of VEGF-A_{165}a resulted in conflicting data, we investigated if ANG2 or this factor in combination with VEGF-A_{165}a affects the barrier formed by iBREC, the well-established model system of immortalized microvascular EC of the bovine retina (Peters et al., 2007; Rangasamy et al., 2011; McCann et al., 2023; Deissler et al., 2005). We have previously shown by continuous electric cell-substrate impedance measurements with a microelectronic biosensor system, i.e. determination of the so-called cell index (CI), that – similar to the behavior of HuREC – 2.5 nM VEGF-A_{165}a induce a severe impairment of the barrier formed by iBREC, an effect evident after a few hours and lasting for days (Sun et al., 2012; Deissler et al., 2017, 2020a, 2022; McCann et al., 2023). Elevated permeability is accompanied by lower expression of the tight-junction (TJ) protein claudin-1, and by subcellular re-localization of TJ-protein claudin-5 and adherens junction (AJ) protein vascular endothelial cadherin (VEcadherin) (Deissler et al., 2011, 2020a, 2022; Wisniewska-Kruk et al., 2012; Dejana et al., 2009; Suarez et al., 2014). By monitoring the cell index as a measure of permeability, we now investigated the potential of ANG2 to directly impair the iBREC barrier or to modulate the VEGF-A_{165}a-induced disturbance. We also studied potential effects on expression and/or subcellular localization of proteins involved in regulation of paracellular flow, i.e. TJ-proteins claudin-1 and claudin-5, and AJ-protein VEcadherin. Because ANG2 interacts with subunit integrin α5 of the fibronectin receptor integrin α5β1 that is crucially involved in the interaction of iBREC with the extracellular matrix, this protein was also included in our analyses (Kanchanawong and Calderwood, 2023; Deissler et al., 2022).

In view of potential implications on therapy with VEGF-binding proteins we further investigated whether inhibition of only VEGF-A-driven signaling is sufficient to prevent barrier disturbance induced in concert by both growth factors. In these experiments either interaction between VEGF-A_{165}a and its receptor(s) was blocked with the VEGF-A-binding humanized antibody bevacizumab, or the tyrosine kinase activity of VEGFR1/2 was inhibited with tivozanib (Presta et al., 1997; Nakamura et al., 2006; Deissler et al., 2012, 2017). The bi-specific

Table 1
Primary and secondary antibodies.

Target	Host, Type and Conjugate	Source[a)]	Working Concentrations	
actin	mouse, monoclonal	clone 5J11, Novus Biologicals, #NBP2-25142	WB:	700 ng/ml
ANG2[b)]	goat, polyclonal	bio-techne, #AF623	WB:	1:200
integrin α5	rabbit, polyclonal	abcam, #ab112183	WB:	0.5–1 μg/ml
claudin-1	rabbit, polyclonal	Invitrogen, #51-9000	WB:	0.25 μg/ml
claudin-5	rabbit, polyclonal	Invitrogen, #34-1600	WB:	100 ng/ml
VEcadherin	rabbit, polyclonal	Cell Signaling Technology B.V., #2158S	WB:	1:1000
			IF:	1:100
VEGF-A	goat, polyclonal	bio-techne, #AF1603	WB:	1:2000
whole IgG, rabbit	goat, polyclonal, coupled to HRP*)	Biorad, #170-5046	WB:	1:30000
whole IgG, mouse	goat, polyclonal, coupled to HRP*)	Biorad, #170-5047	WB:	1:30000
IgG, γ-chain, human	goat, polyclonal, coupled to HRP*)	Thermo Fisher Scientific, #62-8420	WB:	1:1000
IgG, H + L chains, goat	donkey, polyclonal, coupled to HRP*)	bio-techne, #HAF109	WB:	1:4000
IgG, H + L chains, rabbit	goat, F(ab')$_2$ fragment, coupled to AlexaFluor595	Invitrogen, #A11072	IF:	1:500

[a)] abcam, Cambridge, UK; Biorad, Munich, Germany; bio-techne, Wiesbaden, Germany; Cell Signaling Technology B.V., Frankfurt, Germany; Invitrogen via Thermo Fisher Scientific, Schwerte, Germany; Novus Biologicals via bio-techne.

[b)] ANG2, angiopoietin-2; VEcadherin, vascular endothelial cadherin, VEGF, vascular endothelial growth factor; HRP, horseradish peroxidase; IF, immunofluorescence stainings; WB, Western blot analyses.

antibody faricimab was also included in our studies to figure out if targeting both VEGF-A and ANG2 is superior in our experimental setting (Regula et al., 2016).

2. Material and Methods

2.1. Antibodies and reagents

Table 1 contains all relevant information on the antibodies used in this study. The humanized VEGF-A-binding antibody bevacizumab (Avastin, Roche Pharma, Grenzach-Wyhlen, Germany, or VEGzelma, Celltrion Healthcare Hungary, Budapest, Hungary; 25 mg/ml in 50 mM sodium phosphate, 6% α,α-trehalose dihydrate, 0.04% polysorbate 20, pH 6.2) was initially repackaged into syringes at the pharmacy of the University Hospital Giessen and Marburg (Presta et al., 1997). After transfer to inert plastic vials, it was stored in the laboratory at 4 °C for a period not exceeding two months. Faricimab, a bi-specific antibody efficiently binding to ANG2 and to all splice variants of VEGF-A (Vabysmo; 120 mg/ml in 3.1 mg/ml L-histidine, 1.044 mg/ml L-methionine, 1.46 mg/ml NaCl, 54.8 mg/ml D-sucrose, 0.04% polysorbate 20, pH 5.5) was purchased from Roche Pharma (Regula et al., 2016). Tivozanib (Selleckchem, Absource Diagnostics, Munich, Germany) inhibits the tyrosine kinase activities of VEGFR1, VEGFR2 or VEGFR3 at 30 nM, 6.5 nM or 15 nM, respectively, of platelet-derived growth factor receptors α and β at 40 nM and 49 nM, respectively, and of c-kit at 49 nM (Nakamura et al., 2006). The inhibitor was dissolved in dimethyl sulfoxide (Merck, Darmstadt, Germany) to result in final solvent concentrations below 0.05% in the cell culture medium which did not affect morphology or behavior of iBREC (Deissler et al., 2017, 2020a). Recombinant human *Sf*21-expressed VEGF-A_{165}a (#293VE) and recombinant human ANG2 (#623-AN) expressed in the murine myeloma cell line NS0 were purchased from bio-techne. VEGF-A_{165}a (final concentration: 100 μg/ml) was dissolved in phosphate-buffered saline without Ca^{2+} and Mg^{2+} (PBSd; Thermo Fisher Scientific), ANG2 (final concentration: 200 μg/ml) in phosphate-buffered saline (PBS; Thermo Fisher Scientific) containing 0.1% bovine serum albumin (BSA; fraction V, Serva Electrophoresis GmbH, Heidelberg, Germany); both growth factors were stored at −80 °C for no longer than three months.

2.2. Cultivation of iBREC

Telomerase-immortalized microvascular endothelial cells from bovine retina (iBREC) – established in our laboratory – were cultivated on surfaces coated with fibronectin (50 μg/ml in PBSd; Corning, Amsterdam, The Netherlands) in ECGM-1 as described in detail elsewhere (Deissler et al., 2005, 2020a; Busch et al., 2021). Cell culture media ECGM-1, ECGM-2 and ECGM-3 used for culture maintenance or experiments, respectively, were prepared as shown in Table 2 by supplementation of Endothelial Cell Growth Medium MV (ECGM; #C-22120, Promocell, Heidelberg, Germany) containing 1 g/l glucose. Supplements were purchased from Promocell with the exception of geneticin from Thermo Fisher Scientific. Cells were used from passages 25 to 60 counting from the stage of primary culture for which we have confirmed stable expression of proteins specific for microvascular EC, e.g. claudin-5, von Willebrand factor, as well as of proteins under investigation (Kluger et al., 2014; Deissler et al., 2017, 2022). To ensure authenticity of the cells, their characteristic proliferation profile was also routinely recorded by measurements of the electric cell-substrate impedance with the microelectronic biosensor system for cell-based assays xCELLigence RTCA DP (Agilent, OLS, Bremen, Germany) (Deissler et al., 2005, 2017).

2.3. General information

If not stated otherwise, a final concentration of 250 μg/ml (~2 μM) was chosen for faricimab, and bevacizumab, which is achievable by intravitreal injection (Wells et al., 2015; Wong et al., 2023). To avoid unspecific effects of tivozanib, it was used at concentrations of 10 nM or 100 nM close to its published IC50 (Nakamura et al., 2006). In addition, 10 nM tivozanib efficiently prevent the VEGF-A_{165}a-induced dysfunction of a barrier formed by an iBREC monolayer (Deissler et al., 2017). VEGF-A_{165}a was used at concentrations of 2.5 ng/ml (~0.13 nM), 25 ng/ml (~1.25 nM) or 50 ng/ml (~2.5 nM) and ANG2 at concentrations of 25 ng/ml (~0.4 nM), 50 ng/ml (~0.8 nM) or 200 ng/ml (~3 nM) as described below. In control experiments, cells were always processed in exactly the same way in cell culture medium only lacking the effector(s) investigated.

2.4. Assessment of iBREC proliferation by cell index measurements

The proliferation of iBREC in the presence of ANG2 was assessed by continuous electric cell-substrate impedance measurements with the microelectronic biosensor systems for cell-based assays xCELLigence RTCA DP. In each individual well of an E-Plate 16 PET (Agilent) impedance was measured every 15 min between gold electrodes at the beginning of an experiment (Z_0) and at individual time points (Z_i) thereafter, and expressed as the unit-free parameter cell index $CI=(Z_i-Z_0)/15\ \Omega$ (RTCA Software Pro version 2.6.1, Agilent) (Sun et al., 2012). As each E-Plate 16 PET has sixteen individual wells and up to three E-Plates can be measured in parallel, a total of 48 wells can be individually assessed in an experiment. Cells (~10^3 per fibronectin-coated well) were cultured in ECGM-2 for 24 h and then in serum-free ECGM-3 (see Table 2 for details). After further incubation for two days, the cell culture medium was completely replaced by ECGM-2 supplemented with ANG2 to get final concentrations of 0.4–3 nM. At the end of experiments two days later, recorded CI values ($n \geq 5$ for each condition and time point) were normalized (RTCA Software Pro version 2.6.1, Agilent) in relation to those measured immediately before placing the cells in ANG2-containing cell culture medium, and the results were converted to graphs showing means and standard deviations with Graph Pad Prism 9.4.1 (Graph Pad Software, San Diego, USA).

Table 2
Compositions of cell culture media.

Name	Basal cell culture medium	Supplements added						
		Geneticin [μg/ml]	ECGS[a)] [%]	Heparin [μg/ml]	FBS[a)] [%]	Hydrocortisone [nM]	hEGF[a)] [ng/ml]	Fibronectin [μg/ml]
ECGM-1	Endothelial Cell Growth Medium MV containing 1 g/l glucose	300	0.4	90	5	100	10	0
ECGM-2		300	0.4	90	5	100	0	1
ECGM-3		300	0.4	90	0	100	0	1

[a)] ECGS: Endothelial Cell Growth Supplement; FBS: fetal bovine serum; hEGF: human epidermal growth factor.

2.5. Cell index measurements indicative of barrier stability

As a measure of stability of the barrier formed by a monolayer of iBREC we monitored the cell index with the xCELLigence RTCA DP system as previously described (Deissler et al., 2017, 2022). Briefly, ~10^4 cells per fibronectin-coated well were cultured in ECGM-2 until a confluent cell monolayer was reached three to four days later, indicated by a constant and high cell index (CI ~ 20, compared to CI ~ 0 of an empty well). Then, the cell culture medium was replaced with fresh ECGM-2, followed by CI measurements every 15 min. After further incubation for one day, effectors (e.g. VEGF-A_{165}a, ANG2, VEGF-binding proteins or tivozanib, or combinations thereof) were added and the CI was determined every 5 min until the end of the experiments three or six days later. As controls, cells were similarly treated with cell culture medium devoid of effectors. Recorded CI values were normalized in relation to those measured immediately before addition of the effectors, and the results were converted to graphs showing means and standard deviations with Graph Pad Prism 9.4.1 (Deissler et al., 2017, 2022).

2.6. Preparation of protein extracts

Cells were cultivated either on E-plates for CI-measurements (see 2.5) or in fibronectin-coated T25-cell culture flasks (Sarstedt, Nuembrecht, Germany), and exposed to effectors as described above. At the end of each experiment, integrity of the confluent monolayer was confirmed by microscopy and cell culture supernatants were collected and stored at −80 °C for further analyses. Preparation of whole cell extracts started with washing the cells in cold PBS (supplemented with 0.5x EDTA-free Halt Protease Inhibitor Cocktail (#78437, Thermo Fisher Scientific)) which were then suspended in lysis buffer (Lysis buffer 17 (#895943, bio-techne) supplemented with 1x EDTA-free HALT Protease Inhibitor Cocktail and 0.5% Phosphatase Inhibitor Cocktail 2 (#P5726-1 ML, Merck); 10 μl per well of an E-Plate or 100 μl per T25-cell culture flask). After incubation on ice under gentle shaking for 30 min and subsequent centrifugation (18000×*g*, 30 min, 4 °C), the supernatant was collected and stored at −80 °C.

2.7. Western blot analyses of protein extracts

Proteins of relevance to be analyzed by Western blot were separated by gel electrophoresis in 4–20% Mini-PROTEAN TGX Precast Protein Gels (Bio-Rad) and transferred to a polyvinylidene fluoride membrane (Immun-Blot PVDF membrane, Bio-Rad). After incubation in a solution of 1% blocking reagent (#11096176001, Merck) in PBSd with 0.1% Tween-20 (Bio-Rad) for 90 min at room temperature or overnight at 4 °C, membranes were exposed to primary antibodies for 90 min at room temperature, followed by washing in 0.1% Tween-20/PBSd and incubation with corresponding secondary antibodies for 30 min at room temperature. All antibodies were diluted in 0.1% blocking reagent in PBSd with 0.1% Tween-20. The membrane was washed again and treated with Pierce™ ECL Plus Western Blotting-substrate (#32132X3, Thermo Fisher Scientific). Chemiluminescence signals were then directly scanned with the imaging system Fusion FX6 Edge V0.7 (Vilber Lourmat, Eberhardzell, Germany).

To quantify the signals, peak volumes of the protein-specific bands (≥ four replicates) determined with EvolutionCapt Edge software (Version 18.12; Vilber Lourmat) were first set in relation to those of actin in the very same sample. Signals were then normalized to those obtained from similarly processed control cells that had not been exposed to effectors. To quantify VEGF-A or faricimab after treatment of cells with effectors, their signals were normalized to those obtained from cells exposed only to VEGF-A or faricimab, respectively (Deissler et al., 2022). Only to analyze the dimer of VEGF-A, proteins were not reduced prior to electrophoretic separation, otherwise reducing conditions were applied. To allow re-exposure to antibodies with other specificity, membranes were stripped by incubation in Restore Plus Western Blot Stripping Buffer (#46430, Thermo Fisher Scientific) for 45 min at room temperature. After washing three times for 5 min with 0.1% Tween-20/PBSd, membranes were incubated with blocking solution and subsequently with appropriate primary and secondary antibodies as described above (Busch et al., 2021). Normalized data from multiple Western-blots with several independently prepared cell extracts were pooled and presented along with means and standard deviations as scatter plots, in which each dot represents a single signal from one Western blot analysis.

2.8. Immunofluorescence staining

Cells were cultured as described above on fibronectin-coated two-chamber slides (#94.6140.202, x-well PCA Tissue Culture Chambers; Sarstedt) until a confluent monolayer was reached. Then the cell culture medium was replaced by 1.5 ml ECGM-2 per well and one day later effectors were added. After further incubation for one day, cells were fixated in methanol for 7.5 min at −20 °C, immunostained with antibodies directed against VEcadherin (see Table 1) as described in detail elsewhere, and examined by fluorescence microscopy (BZ-X810 microscope, Keyence Deutschland GmbH, Neu-Isenburg, Germany) (Deissler et al., 2020a, 2020b, Busch et al., 2021). Cells with a homogenous and continuous plasma membrane staining and minimal intracellular staining defined as VEcadherin-positive were manually counted in at least four randomly chosen microscopic fields each containing ~300 cells.

2.9. Determination of VEGF-A and ANG2 by ELISA

The Quantikine ELISA Canine VEGF-A Immunoassay Kit (#CAVE00, bio-techne) was used to determine VEGF-A in cell culture supernatants or cell extracts from ~10^5 iBREC that had been exposed to VEGF-A_{165}a and/or ANG2 in combination with bevacizumab, faricimab or tivozanib. Samples were diluted 1:5 in PBSd (supernatants of cells exposed to 2.5 nM VEGF-A_{165}a/3 nM ANG2/2 μM bevacizumab or faricimab) or diluted 1:100 in PBSd (all other supernatants and all cell extracts) (Deissler et al., 2017, 2020b, 2022). ANG2 – possibly present in cell culture supernatants or cell extracts – was determined with the Human Angiopoietin-2 Quantikine ELISA Kit (#DANG20, bio-techne). Samples were diluted 1:100 with PBSd, with the exception of supernatants obtained from unchallenged or VEGF-A_{165}a-treated iBREC. ANG1 – possibly secreted by iBREC exposed to VEGF-A_{165}a, ANG2 or combinations thereof – was measured in samples of undiluted cell culture supernatants with the Porcine Angiopoietin-1 ELISA Kit (#ES1RB, Thermo Fisher Scientific). Assays were performed by processing duplicate samples according to the manufacturers' instructions. Analyte-dependent absorbance was measured at 450 nm (reference wavelength: 570 nm) 15–20 min after addition of the stop solution with an Infinite 200Pro spectrophotometer controlled by I-control software (Tecan, Crailsheim, Germany) (Deissler et al., 2022). Standard curves to quantify human VEGF-A (0–1250 pg/ml; minimal detectable dose: 20 pg/ml), human ANG2 (0–3000 pg/ml; minimal detectable dose: 47 pg/ml) or porcine ANG1 (0–15000 pg/ml; minimal detectable dose: 61 pg/ml) were always generated in parallel to the analyses of samples.

In order to confirm that binding of faricimab to ANG2 and VEGF-A_{165}a does not affect the interaction of ANG2 with the detection antibodies of the ELISA kit used, mixtures containing 2.5 nM VEGF-A_{165}a, 3 nM ANG2 and 20 nM-2 μM faricimab were incubated for 15 min at room temperature to allow formation of the ANG2/faricimab/VEGF-A_{165}a complex. Then samples were diluted 1:100 in PBSd and processed as described above.

2.10. Statistical analyses

All experiments were performed at least three times. To compare antigen-specific Western blot signals from effector-treated cells to the hypothetical value of 1.00 of normalized signals from cells not exposed

to effectors studied, we used the One-sample *t*-test, which takes into account that there is variation of the standard deviation although it appears to be zero in the calculations or graphs. The Mann-Whitney *U* test was applied when two groups of antigen-specific Western blot signals from differently treated cells were compared, the one-way analyses of variance (ANOVA) followed by Tukey's test to compare several groups. ANOVA followed by Tukey's test was also used to compare antigen-specific absorbances from ELISA. Measured CI values were analyzed with two-way ANOVA followed by Šídák's multiple comparison test. Differences resulting in p-values below 0.05 were considered

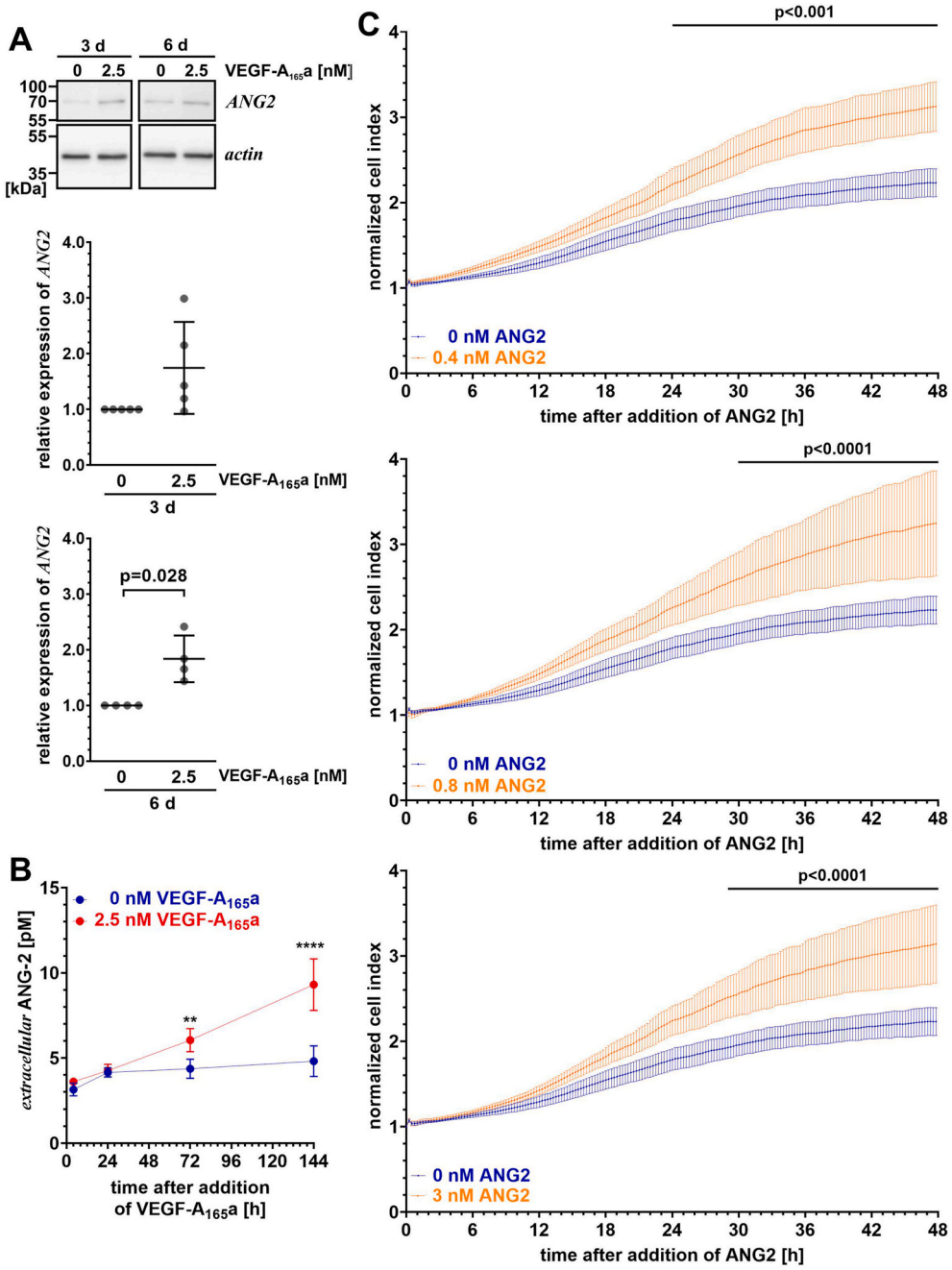

Fig. 1. ANG2 enhanced proliferation of iBREC

(A) Confluent monolayers of iBREC were exposed to 2.5 nM VEGF-A_{165}a for three or six days, respectively, before cells were harvested for preparation of cell extracts. ANG2-specific signals of Western blot analyses were normalized as described in Material and Methods. Scatter blots show means and standard deviations, and one dot represents the ANG2-specific signal from one of multiple independent Western blot analyses. Levels of ANG2 were higher after extended exposure to VEGF-A_{165}a. (B) Cell culture supernatants obtained from confluent iBREC exposed to 2.5 nM VEGF-A_{165}a for up to six days were collected at indicated time points for determination of ANG2 amounts by ELISA. Graph shows means and standard deviations; n = 6 for each condition and time point. Data were analyzed with two-way ANOVA followed by Šídák's multiple comparison test. More ANG2 is present in the cell culture supernatant after extended exposure to VEGF-A_{165}a. (C) ANG2 was added to serum-arrested, non-confluent iBREC and the CI was recorded continuously as a measure of proliferating cells as described in Material and Methods. CI values were obtained from at least five wells per condition and time point, were normalized in relation to those measured just before the addition of the growth factor, and are shown as means ± standard deviations. The increase of the CI indicates that ANG2 enhances proliferation of iBREC compared to unchallenged cells. If not mentioned otherwise, data were analyzed as described in "2.10 Statistical analyses". **) $p < 0.01$, ****) $p < 0.0001$ compared to control, indicating only statistically significant differences.

significant. All statistical analyses were performed with Graph Pad Prism 9.4.1; means and standard deviations are provided as numbers, graphs or in scatter plots.

3. Results

3.1. ANG2 enhanced proliferation of iBREC

Unchallenged iBREC expressed very low amounts of ANG2, which were significantly higher after exposure of the cells to VEGF-A_{165}a for six days, as revealed by Western blot analyses of whole cell extracts (Fig. 1A). The very low levels of ANG2 measured in the cell culture supernatant of unchallenged iBREC – not higher than those measured in cell culture medium without cells (4.5 ± 0.1 pM ANG2; N = 4) – also slightly, but significantly increased during exposure with VEGF-A_{165}a for up to six days (Fig. 1B). In contrast, iBREC exposed to VEGF-A_{165}a did not secrete any ANG1.

All experiments aiming at possible responses of iBREC to ANG2 were carried out with recombinant *human* ANG2. Due to the high degree of similarity between the *bovine* and *human* homologues of both the growth factor and its receptor Tie2, binding of the *human* ANG2 to the *bovine* receptor and subsequent induction of signal transduction could be expected (Barton et al., 2006). This plausible assumption was confirmed by verifying if recombinant human ANG2 was able to enhance proliferation of non-confluent iBREC. Therefore, iBREC were seeded at a low density and cultured in serum-free cell culture medium for two days before they were treated with 0.4 nM–3 nM ANG2 in serum-containing cell culture medium. Within 16 h the continuously measured CI started to increase and the rise was significantly higher when cells were exposed to ANG2 (Fig. 1C). This finding confirms that *human* ANG2 can indeed induce signal transduction in *bovine* REC associated with stimulation of proliferation.

3.2. Function of the iBREC barrier was not altered by ANG2

As a measure of barrier function, we determined the CI of a confluent iBREC monolayer exposed for several days to concentrations of ANG2 that are sufficient to stimulate iBREC proliferation, but the curves

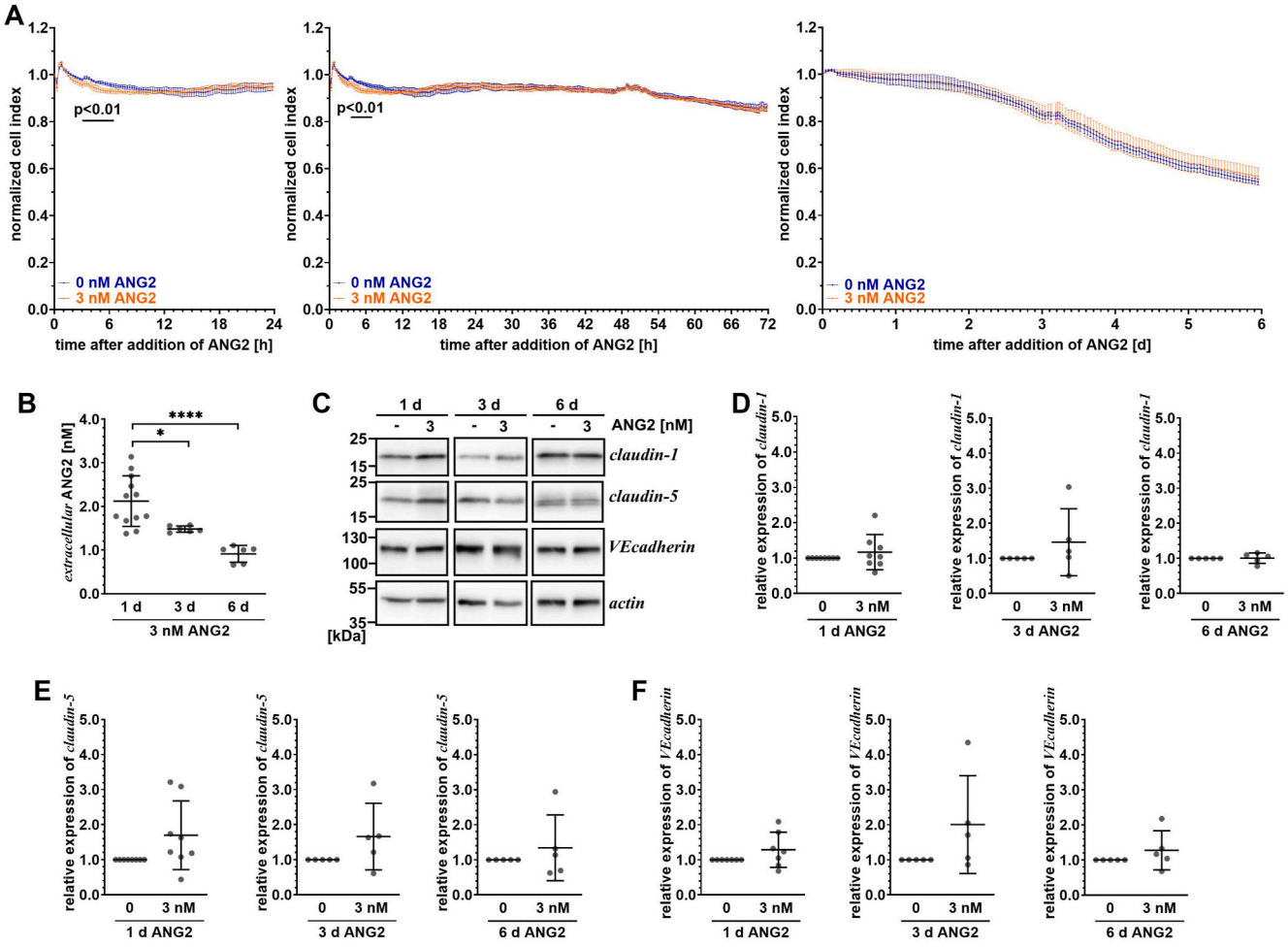

Fig. 2. ANG2 did not persistently impair the barrier formed by iBREC

Confluent iBREC were cultivated without (n = 6) or treated with 3 nM ANG2 (n = 6) for several days and (A) the CI was measured continuously, (B) amounts of ANG2 in the cell culture supernatant were determined by ELISA at indicated time points or (C–F) cells were harvested for preparation of cells extracts at indicated time points and subsequent Western-blotting. (A) CI values were normalized in relation to those measured just before the addition of the ANG2, and are shown as means ± standard deviations. ANG2 did not persistently change the CI in comparison to that of unchallenged cells despite subtle and transient changes evident within 18 h after its addition. (B) Scatter plots of pooled ELISA data (N ≥ 6 per time point and condition) obtained from several independently acquired cell culture supernatants depict means and standard deviations. Amounts of ANG2 in the cell culture supernatant declined over time. (C–F) Amounts of TJ-proteins claudin-1 and claudin-5, and of AJ-protein VEcadherin were not changed after exposure to ANG2. Specific signals of Western blot analyses were normalized as described in Material and Methods. Scatter blots show means and standard deviations of pooled Western blot data, and one dot represents the analyte-specific signal from one of multiple independent Western blot analyses. Data were analyzed as described in "2.10 Statistical analyses". *) $p < 0.05$, ****) $p < 0.0001$, indicating only statistically significant differences.

obtained from unchallenged and treated cells were congruent (Fig. 2A). Only around 6 h after addition of 3 nM ANG2 the CI was significantly lower (Fig. 2A), but this subtle and transient effect was leveled during further incubation (Fig. 2A). Similarly, 0.4 nM or 0.8 nM ANG2 did not significantly affect the CI during exposure for three days (Supplementary Fig. 1). Over the incubation time ANG2 decreased in the cell supernatants, but not below 0.8 nM, a concentration sufficient to stimulate iBREC proliferation (Fig. 2B). In accordance with the observation of a stable barrier, iBREC exposed to ANG2 did not secrete substantial amounts of VEGF-A_{165}a above the detection limit of the ELISA used. Because action of ANG2 might be counteracted by ANG1 we also determined this potentially secreted growth factor in cell culture supernatants of iBREC exposed to 0.4 nM–3 nM ANG2, but relevant amounts of ANG1 were not detected. Expression of proteins involved in the regulation of barrier function, e.g. TJ-proteins claudin-1 (Fig. 2C and D), claudin-5 (Fig. 2C–E) and AJ-protein VEcadherin (Fig. 2C–F), also remained stable during extended exposure of the cells to ANG2. Furthermore, treatment with 3 nM ANG2 for one day did not change portion of cells with the typical subcellular localization of VEcadherin at the plasma membrane in unchallenged iBREC (Fig. 5A and B).

3.3. ANG2 enhanced barrier dysfunction induced by low concentrations of VEGF-A_{165}a

Because of the hypothesis that ANG2 might modulate the changes induced by VEGF-A_{165}a, we exposed confluent monolayers of iBREC for up to three days to increasing concentrations of VEGF-A_{165}a (0.13 nM–2.5 nM) with or without 3 nM ANG2, and continuously measured the CI (Fig. 3A–C). As previously observed, 0.13 nM VEGF-A_{165}a did not change the CI by itself (Fig. 3A, middle panel). The combination of both growth factors, however, subtly and transiently lowered the CI within the first hours after their addition (Fig. 3A, lower panel). Interestingly, ANG2 strongly, albeit transiently enhanced the weak decline of the CI induced by 1.25 nM VEGF-A_{165}a (Fig. 3B), and the strong and persistent decline of the CI induced by 2.5 nM VEGF-A_{165}a (Fig. 3C, middle panel) was only slightly and transiently amplified by ANG2 (Fig. 3C, lower panel). Because the more pronounced response of iBREC might possibly be due to higher secretion of VEGF-A induced by ANG2, we measured by ELISA the concentration of this growth factor in the supernatant of iBREC exposed to VEGF-A_{165}a ± ANG2 (Table 3). After treatment for one day with 0.13 nM VEGF-A_{165}a, the amount of VEGF-A was very low and not detectable at all after three days; levels were not modulated by

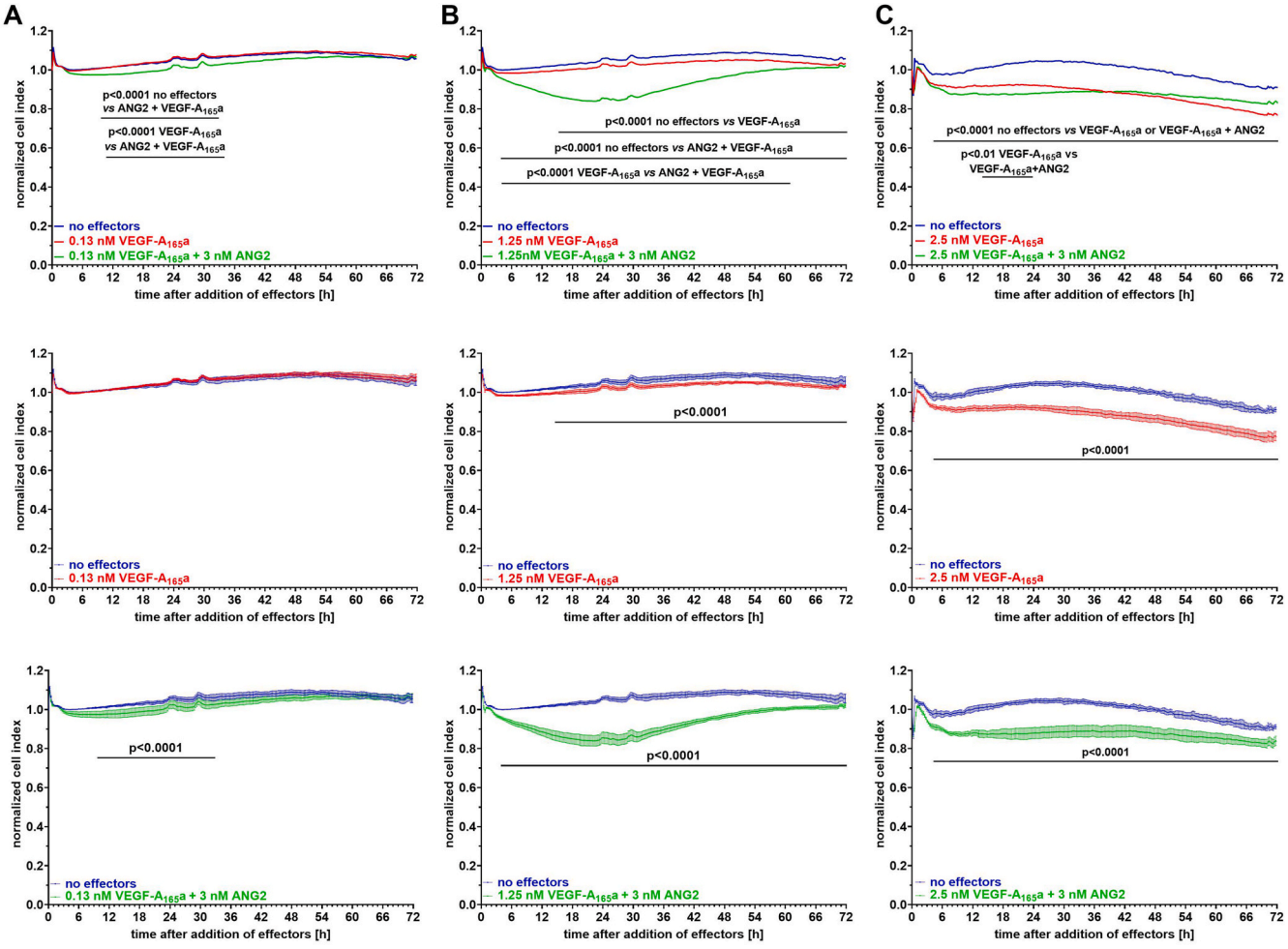

Fig. 3. ANG2 enhanced the VEGF-A_{165}a-induced decline of the CI
Confluent monolayers of iBREC were exposed to 0.13 nM–2.5 nM VEGF-A_{165}a with or without 3 nM ANG2 for up to three days and the CI was measured continuously. CI values were normalized in relation to those measured just before the addition of the growth factors. To give an overview of observed changes, the means are provided in the upper graphs; the middle and lower graphs show means ± standard deviations. (A) 0.13 nM VEGF-A_{165}a (n = 7) did not change the CI in comparison to unchallenged iBREC (n = 7; middle panel), but the combination of 0.13 nM VEGF-A_{165}a +3 nM ANG2 (n = 8) subtly and transiently lowered the CI (lower panel). (B) The weak, but significant decline of the CI induced by 1.25 nM VEGF-A_{165}a (n = 7; middle panel) was significantly amplified by 3 nM ANG2 (n = 8; lower panel). (C) ANG2 (n = 7; lower panel) slightly enhanced the persistent and strong decline of the CI induced by 2.5 nM VEGF-A_{165}a (n = 7; middle panel). Data were analyzed as described in "2.10 Statistical analyses"; only statistically significant differences are indicated.

Table 3
Concentrations of VEGF-A measured in supernatants of iBREC exposed to VEGF-A_{165}a ± ANG2.

growth factor combination	concentration of VEGF-A in cell culture supernatant [nM]					
	exposure for 1 d			exposure for 3 d		
	mean ± SD	N	p	mean ± SD	N	p
0.13 nM VEGF-A_{165}a	0.16 ± 0.10	8	<0.05	not detected	6	
0.13 nM VEGF-A_{165}a +3 nM ANG2	0.09 ± 0.09	8		not detected	7	
1.25 nM VEGF-A_{165}a	0.83 ± 0.03	8	<0.05	0.55 ± 0.20	16	<0.05
1.25 nM VEGF-A_{165}a +3 nM ANG2	0.95 ± 0.20	8		0.58 ± 0.10	10	
2.5 nM VEGF-A_{165}a	2.30 ± 0.10	8	<0.05	1.70 ± 0.10	5	<0.05
2.5 nM VEGF-A_{165}a +3 nM ANG2	2.20 ± 0.20	8		1.60 ± 0.10	5	

Confluent iBREC were incubated with growth factors for one or three days before cell culture supernatants were harvested. Then the oncentration of VEGF-A was measured by ELISA. Pooled ELISA data of several independently acquired cell culture supernatants are shown as means and standard deviations (SD).

ANG2. ANG2 also did not enhance the amount of VEGF-A in the supernatant of cells exposed to 1.25 nM or to 2.5 nM VEGF-A_{165}a.

Amounts of proteins involved in the regulation of barrier stability were found to be differently changed after treatment with VEGF-A_{165}a: Significantly less claudin-1 was observed one day after addition of VEGF-A_{165}a (Fig. 4A), but two days later, expression of the TJ-protein remained lower only after treatment with ≥1.25 nM VEGF-A_{165}a (Fig. 4B). Prolonged exposure to VEGF-A_{165}a for three days resulted in slightly, but significantly more claudin-5 and VEcadherin (Fig. 4B). Additional exposure to ANG2 did not significantly modulate VEGF-A_{165}a-induced changes.

Exposure of iBREC to VEGF-A_{165}a (1.25 nM or 2.5 nM) for one day dramatically changed the morphology of the cells: The typical cobblestone shape was lost and cells had become more elongated with foci spanning neighbor cells; these changes were more pronounced at the higher concentration of the growth factor. Accordingly, the typical homogenous and continuous distribution of VEcadherin over the plasma membrane (Fig. 5A, yellow arrows) became significantly more irregular in a concentration-dependent manner (Fig. 5A, yellow arrowheads). Interestingly, ANG2 significantly enhanced the weaker effect of 1.25 nM VEGF-A_{165}a (Fig. 5A–C).

3.4. Inhibition of VEGF-A-driven signaling efficiently prevented barrier dysfunction induced by prolonged treatment with VEGF-A_{165}a plus ANG2

Because ANG2 only subtly enhanced VEGF-A_{165}a-induced barrier dysfunction, inhibition of VEGF-A-driven signaling might be sufficient to prevent the low CI – assessed as a marker of barrier function – caused by 2.5 nM VEGF-A_{165}a together with 3 nM ANG2. Indeed, blocking of the tyrosine kinase activities of the VEGF receptors with 10 nM and 100 nM tivozanib entirely prevented the drop of the CI induced by the growth factors when cells were exposed for up to three days to them (Fig. 6A). A similar effect was observed for 2 μM bevacizumab (Fig. 6B) and 2 μM faricimab (Fig. 6C). Both VEGF-binding proteins similarly prevented the decline of the CI induced only by VEGF-A_{165}a (Fig. 6D and E).

As anticipated, the bi-specific antibody faricimab also efficiently prevented the CI drop induced by 1.25 nM VEGF-A_{165}a together with 3 nM ANG2 (Fig. 6F). This was also achieved, though slightly but not significantly delayed by depletion of VEGF-A only with bevacizumab (Fig. 6G) or by inhibiting the VEGFR2 with 10 nM tivozanib (Fig. 6H).

Low expression of the TJ-protein claudin-1 observed after exposure of iBREC to VEGF-A_{165}a plus ANG2 for three days was similarly prevented by inhibition of VEGF-driven signaling with tivozanib (Fig. 7A), bevacizumab (Fig. 7B), or targeting both growth factors with faricimab (Fig. 7B). Astonishingly, amounts of claudin-5 and VEcadherin were significantly higher after exposure of iBREC to the growth factors together with the inhibitors but not after treatment with the growth factors alone.

3.5. Faricimab prevented uptake of ANG2 by iBREC during prolonged treatment with VEGF-A_{165}a plus ANG2

We also investigated whether extra- and intracellular concentrations of VEGF-A and ANG2 were altered by blocking VEGF-A-driven signaling or by direct effects of the VEGF antagonists. As previously observed, iBREC did not secrete relevant amounts of VEGF-A. Inhibition the tyrosine kinase activities of the VEGF receptors significantly lowered extracellular concentrations of added VEGF-A, whereas intracellular levels were higher compared to cells exposed to the growth factor combination only (Fig. 8A). As anticipated, extracellular as well as intracellular amounts of added ANG2 were not changed by inhibition of the VEGF receptors (Fig. 8B).

In order to study whether VEGF-A_{165}a is completely bound to the VEGF-binding proteins we used ELISA detection antibodies which interact with the same region of the growth factor as the antagonists, so that only free VEGF-A is detected (Muellerleile et al., 2019; Walz et al., 2016). Only very low amounts of free VEGF-A, were present in the supernatants and cell extracts when iBREC had been exposed to the growth factors together with the VEGF antagonists. These VEGF-A levels were particularly low when growth factor-exposed cells had also been treated with faricimab (Fig. 8C). Significantly more unbound VEGF-A was also measured in cell extracts of growth factor-exposed cells treated with bevacizumab compared to those exposed to faricimab (Fig. 8C). Western blot analyses under denaturing conditions allows determination of the total amount of VEGF-A because of disruption of the formed growth factor-antagonist complexes. These analyses revealed that slightly, but significantly more VEGF-A was present in the supernatants when growth factor-exposed iBREC were treated with either of the VEGF-binding proteins (Fig. 8D). However, uptake of VEGF-A was not completely prevented, because the growth factor was also detected in cell extracts of similarly treated iBREC (Fig. 8D).

Interestingly, faricimab efficiently prevented uptake of ANG2 by iBREC: Significantly more ANG2 was present in the supernatants of iBREC exposed for three days to VEGF-A_{165}a and ANG2 plus faricimab compared to those of cells treated only with the growth factors (Fig. 8E). This was also observed early after treatment for only 6 h (Fig. 8F), and the effect was even more pronounced after exposure for six days (VEGF-A_{165}a + ANG2: 0.94 ± 0.07 nM ANG2, VEGF-A_{165}a + ANG2 + faricimab: 2.45 ± 1.05 nM ANG2, $n = 8$; $p = 0.0004$). In contrast, only very low amounts of ANG2 were detected in extracts from cells exposed to the growth factors plus faricimab (Fig. 8E). It could not be ruled out that interaction of faricimab with ANG2 and/or VEGF-A might interfere with binding of the ANG2 ELISA detection antibodies. Therefore, we measured ANG2 in the presence of VEGF-A and increasing concentrations of faricimab in a cell-free assay, but determined amounts of ANG2

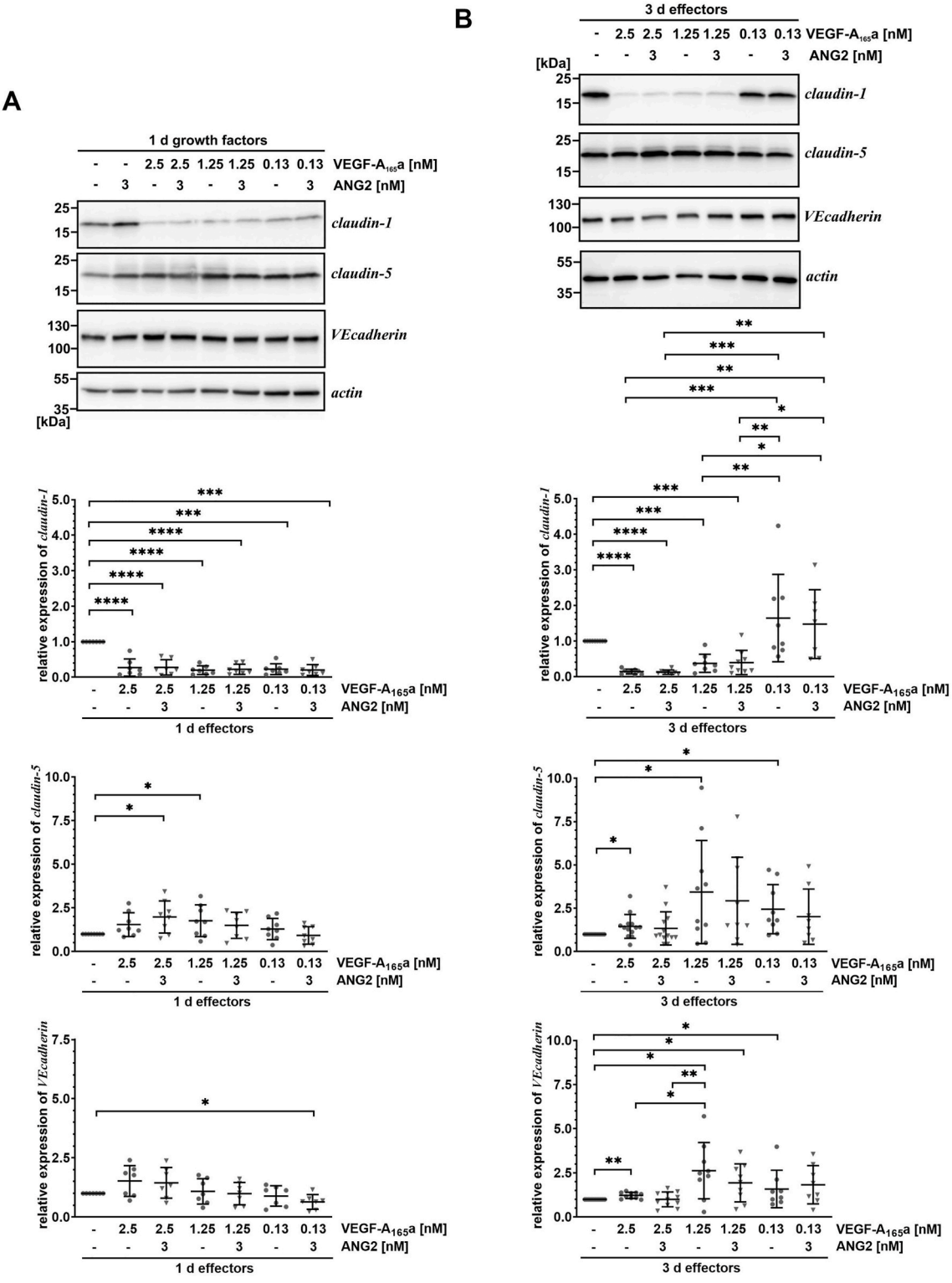

Fig. 4. ANG2 did not modify VEGF-A$_{165}$a-caused lower expression of claudin-1

After establishing a confluent monolayer, iBREC were exposed to 0.13 nM–2.5 nM VEGF-A$_{165}$a in the presence or absence of 3 nM ANG2 for (A) one or (B) three days before cells were harvested for preparation of cell extracts. Specific signals of pooled Western blot analyses were normalized and are presented as scatter blots with means and standard deviations as described in Fig. 2. (A) Amounts of TJ-protein claudin-1 were notably and significantly lower after exposure to VEGF-A$_{165}$a for one day irrespectively of the concentration of the growth factor; ANG2 did not modulate the VEGF-A induced loss. Subtle VEGF-A-induced changes of expression of claudin-5 or of AJ-protein VEcadherin were also not different after additional exposure to ANG2. (C) After exposure for three days, only ≥1.25 nM VEGF-A$_{165}$a significantly lowered protein amounts of claudin-1, those of claudin-5 and VEcadherin were higher; changes were also not modulated by ANG2. Data were analyzed as described in "2.10 Statistical analyses". *) $p < 0.05$, **) $p < 0.01$, ***) $p < 0.001$, ****) $p < 0.0001$, indicating only statistically significant differences.

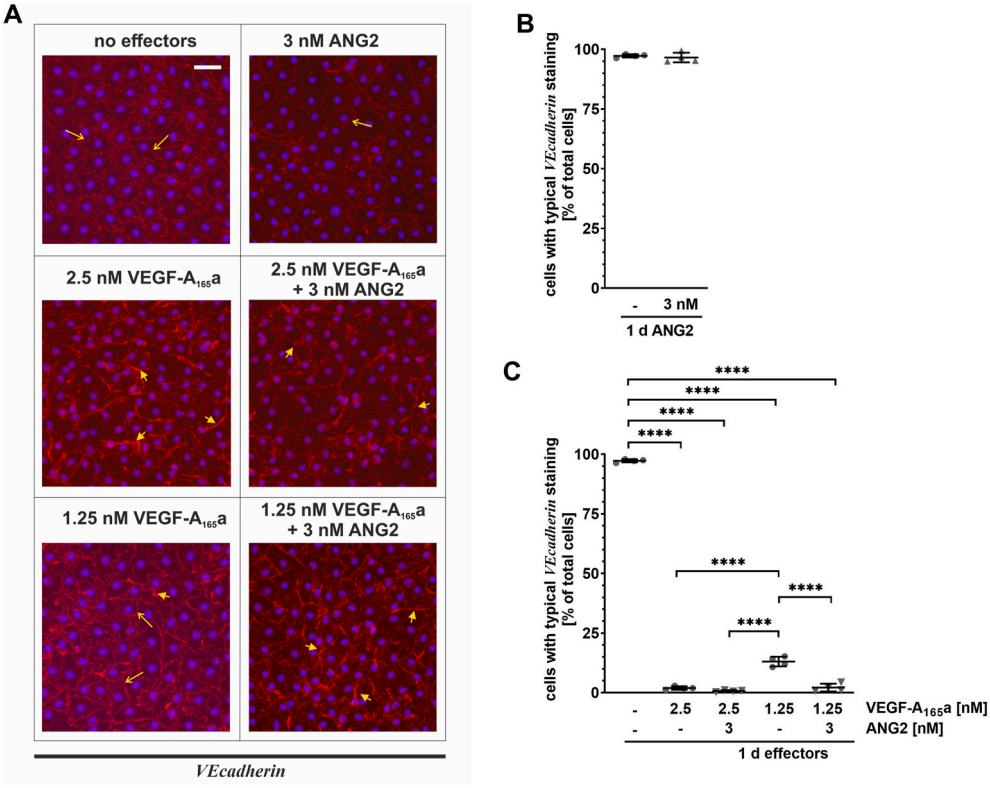

Fig. 5. ANG2 amplified the VEGF-A_{165}a-caused alteration of the subcellular localization of VEcadherin
Confluent iBREC were treated only with 3 nM ANG2, or with 1.25 nM or 2.5 nM VEGF-A_{165}a with or without 3 nM ANG2 for one day before (A) cells were fixated for subsequent immunofluorescence staining with antibodies specific for VEcadherin (→ red); nuclei were stained with 4′,6-diamidino-2-phenylindole (→ blue). (B, C) Cells with the typical continuous and homogenous staining of the plasma membrane (→ yellow arrows) were counted in four different microscopic fields per condition, each with ~300 cells. Typical results of one experiment are shown as scatter blots depicting means and standard deviations. (A) Whereas the strong and homogenous staining at the plasma membrane (→ yellow arrows) was not affected by 3 nM ANG2, it was markedly changed after exposure to VEGF-A_{165}a; significantly less pronounced at the lower concentration: The staining localized at the plasma membrane had become irregular and patchy and was also seen in elongations of the cells (→ yellow arrowheads). Additional treatment with ANG2 significantly enhanced the changes induced by 1.25 nM VEGF-A_{165}a. Data were analyzed as described in "2.10 Statistical analyses". ****) $p < 0.0001$, indicating only statistically significant differences. Scale bar: 50 μm. (For interpretation of the references to colour in this figure legend, the reader is referred to the Web version of this article.)

did not significantly differ from those obtained in the absence of the bi-specific antibody (Fig. 8G).

3.6. Expression of integrin α5 was modulated by VEGF-A_{165}a but not by ANG2

Compromised adhesion to the extracellular matrix can result in a low CI (Jäckle et al., 2020, Deissler et al., 2022a). As such interaction of iBREC is mediated through the fibronectin receptor integrin α5β1, we studied whether extended exposure of iBREC to ANG2 in the presence or absence of VEGF-A_{165}a altered the expression of the subunit integrin α5. In accordance with a stable CI (Fig. 2), expression of integrin α5 was not affected by ANG2 (Fig. 9A). In contrast, exposure of iBREC to ≤1.25 nM VEGF-A_{165}a for one day resulted in a transiently lower expression of integrin α5 (Fig. 9B), but was higher after extended treatment with ≥1.25 nM VEGF-A_{165}a for three days (Fig. 9C). However, additional exposure to ANG2 did not modulate these effects of VEGF-A_{165}a. Neither inhibition of VEGF receptors by tivozanib (Fig. 9D) nor binding of VEGF-A by bevacizumab or of both VEGF-A and ANG2 by faricimab (Fig. 9E) did prevent the stronger expression of integrin α5 after prolonged exposure to VEGF-A_{165}aplus ANG2.

3.7. Prolonged treatment with faricimab stabilized function of the iBREC barrier

Cell index measurements confirmed that prolonged treatment of iBREC over six days with faricimab did not affect the barrier formed by a monolayer of these cells (Fig. 10A). Interestingly, significantly more claudin-1, claudin-5 and VEcadherin were then expressed by the cells, whereas amounts of integrin α5 remained stable (Fig. 10B). Western blot analyses of cell extracts showed that – similar to bevacizumab – faricimab is taken up by the cells: A characteristic double band was observed when samples were separated under reducing conditions (Fig. 10C). This band was significantly more intense when cells had additionally been exposed to the target proteins of faricimab (Fig. 10C and D). Interestingly, cell extracts contained significantly less ANG2 when iBREC had been exposed to VEGF-A_{165}a + ANG2 + faricimab for six days compared to treatment with the growth factors only (Fig. 10E). In contrast, an effect of faricimab on the low amounts of internalized VEGF-A was not observed (Fig. 10F).

4. Discussion

Long-term exposure of primary and immortalized REC to VEGF-A_{165}a results in severe impairment of the barrier formed by this cell type evident a few hours after the growth factor's addition and lasting for several days (Deissler et al., 2011, 2020a, 2022; Wisniewska-Kruk et al., 2016; McCann et al., 2023). This disturbance is indicated by low values of the cell index (CI) or transendothelial electrical resistance (TEER) and accompanied by changes of expression and subcellular localization of TJ-proteins and AJ-proteins (Deissler et al., 2011, 2020a, 2022; Suarez et al., 2014; Wisniewska-Kruk et al., 2016). Maintaining

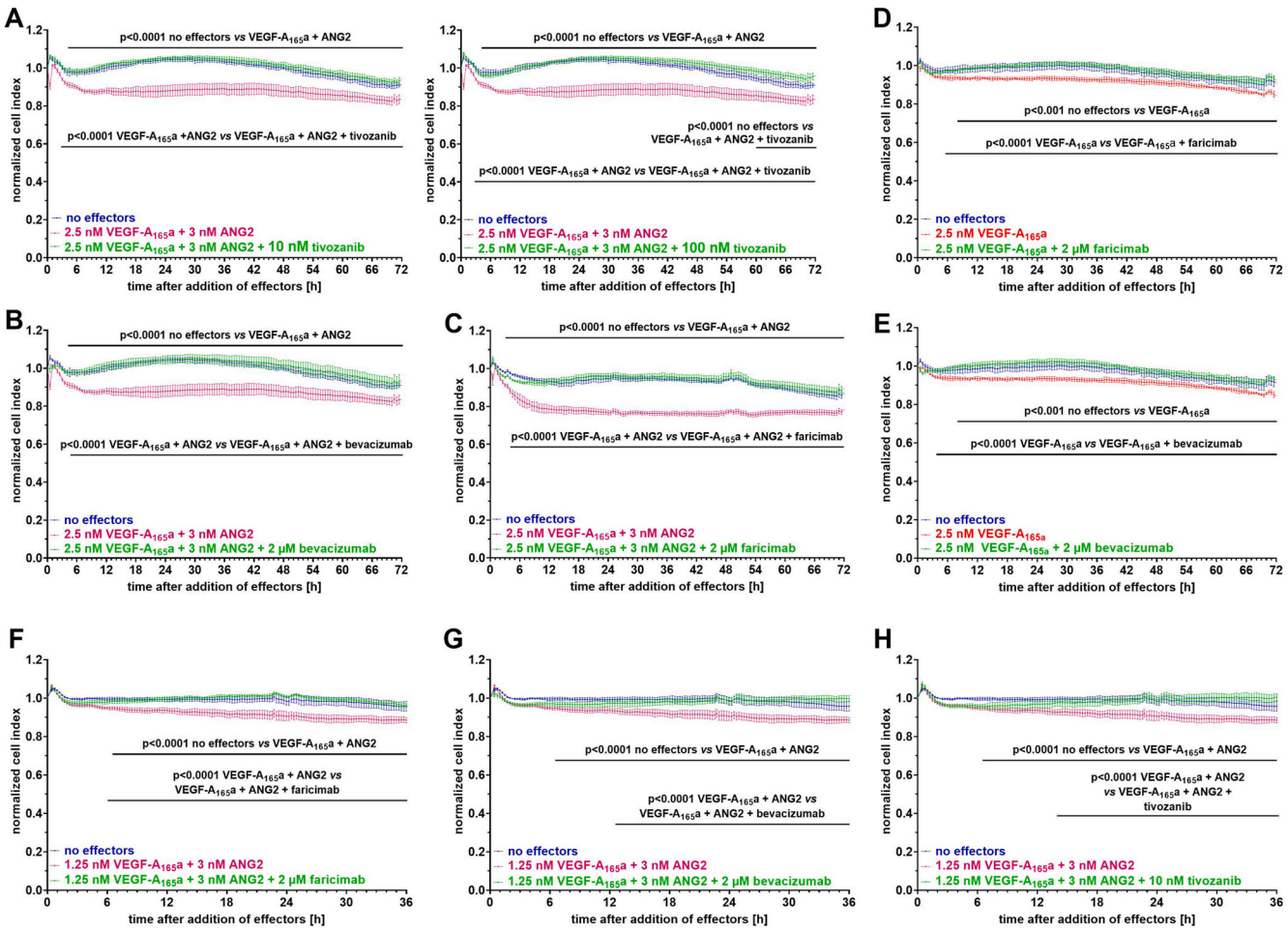

Fig. 6. Blocking of VEGF-A-mediated signaling efficiently prevented reduction of CI induced by extended treatment with VEGF-A$_{165}$a plus ANG2
(A–C) iBREC were exposed to 2.5 nM VEGF-A$_{165}$a +3 nM ANG2 (n = 7) with or without (A) the inhibitor of the VEGF receptor(s) tivozanib (n = 8), (B) bevacizumab (n = 7) or (C) faricimab (n = 7), and the CI was assessed as a measure of permeability. (A) Tivozanib efficiently prevented decline of the CI induced by the growth factor combination; both concentrations were similarly effective. (B) The VEGF-A-binding IgG bevacizumab and (C) the bi-specific antibody faricimab additionally targeting ANG2 also efficiently prevented the low growth factor-induced CI. (D, E) The CI was measured of cells treated with 2.5 nM VEGF-A$_{165}$a (n = 5) with or without (D) faricimab (n = 7) or (E) bevacizumab (n = 7). Both VEGF-A antagonists efficiently prevented VEGF-A-induced decline of the normalized CI. (F–H) Confluent cells were exposed to 1.25 nM VEGF-A$_{165}$a +3 nM ANG2 (n = 5) in the absence or presence of (F) faricimab (n = 8), (G) bevacizumab (n = 6) or (H) tivozanib and the CI was assessed as described above. (F) Faricimab, binding both VEGF-A and ANG2, efficiently prevented the growth factor-induced decline of the CI. This was also observed when VEGF-A-driven signaling was blocked with (G) bevacizumab or (H) tivozanib, although the effect was slightly but not significantly delayed. CI values were always normalized in relation to those measured just before the addition of the effectors, and are shown as means ± standard deviations. Data were analyzed as described in "2.10 Statistical analyses".

the VEGF-A-induced barrier dysfunction over several days only partly depends on VEGF-A-driven signaling, suggesting other permeability inducing factors to be involved (Deissler et al., 2022). One of these could be the angiogenic growth factor ANG2 which is expressed and secreted by (retinal) EC and has been found in the vitreous of DR patients (Watanabe et al., 2005; Kinnunen et al., 2009; Klaassen et al., 2022; Regula et al., 2016; Khan et al., 2020; Rangasamy et al., 2011; Pergolizzi et al., 2018; Eyre et al., 2020; McCann et al., 2023). To investigate if impairment of the barrier formed by REC can be induced or modulated by ANG2 we used the well-established model of iBREC, i.e. telomerase-immortalized bovine REC. This homogeneous cell line is highly authentic as indicated by responses of the cells to stimulation with human growth factors that are similar if not identical to those observed in experiments with primary REC of human and other origins (Castellon et al., 2002; Deissler et al., 2005, 2011; Suarez et al., 2014). That the VEGFR2 is not active in unstimulated iBREC was confirmed in experiments with specific inhibitors that did not affect migration or the formed barrier (Deissler et al., 2013, 2017; Nakamura et al., 2006).

Further confirming similar behavior of HuREC and iBREC, we observed that extended exposure of iBREC to VEGF-A$_{165}$a indeed induces expression and secretion of ANG2 although the achievable concentrations are likely too low to evoke subsequent signaling significantly (Eyre et al., 2020; McCann et al., 2023). However, even at higher exogenous concentrations of added ANG2, the growth factor does not persistently impair the barrier formed by an iBREC monolayer, despite inducing subtle and transient, albeit significant, weakening around 6 h after its addition: The CI remains stable and expression or subcellular localization of claudin-1, claudin-5 or VEcadherin – all involved in the regulation of barrier stability – are not affected during exposure for up to six days. These results are in contrast to published observations that ANG2 itself weakens the barrier formed by a HuREC monolayer (Rangasamy et al., 2011). However; only exposure up to 24 h was previously investigated in the mentioned study under different conditions. Most importantly, various components of cell culture media are known to influence the stability of the barrier and therefore we chose conditions that allow the establishment of a tight barrier by iBREC (Deissler et al., 2011, 2022; Busch et al., 2021). Furthermore, before ANG2 is added, iBREC are also allowed to recover for one day to avoid immediate effects

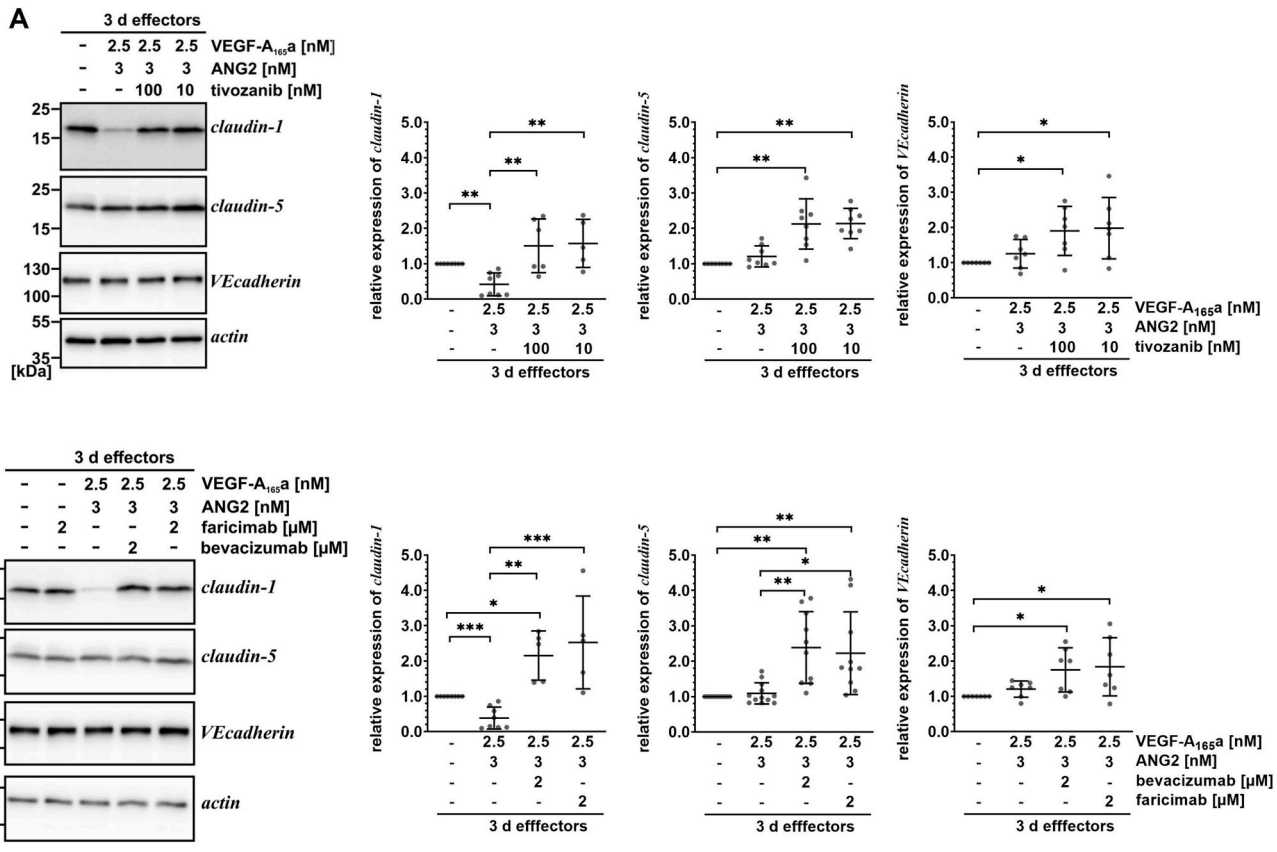

Fig. 7. Inhibition of VEGF-A-driven signaling efficiently prevented lower expression of TJ-protein claudin-1 induced by extended treatment with VEGF-A_{165}a plus ANG2

After treatment of iBREC with VEGF-A_{165}a + ANG2 in the absence or presence of (A) tivozanib, (B) bevacizumab or faricimab, cells were harvested for preparation of cell extracts. Specific signals of Western blot analyses were normalized and are shown as scatter blots with means and standard deviations as described above. (A) Inhibition of VEGF receptor(s) by tivozanib efficiently prevented the loss of TJ-protein claudin-1 induced by growth factor treatment. (B) Similar observations were made in experiments with bevacizumab or faricimab. More claudin-5 and VEcadherin was detected in cell extracts of growth factor-treated iBREC additionally exposed to anyone of the inhibitors tested. Data were analyzed as described in "2.10 Statistical analyses". *) $p < 0.05$, **) $p < 0.01$, ***) $p < 0.001$; only statistically significant differences are indicated.

caused by exchange of the cell culture medium and associated unspecific responses of the cells (Deissler et al., 2020b). As a consequence of optimized conditions, the TEER of the iBREC monolayer (4500 Ω; Deissler, unpublished observations) is at the time of addition of effectors much higher than that described for HuREC (1200 Ω; Rangasamy et al., 2011), suggesting that the tighter iBREC barrier might be less sensitive to ANG2. This hypothesis is confirmed by our observation of a strong and stable VEcadherin-specific staining at the plasma membrane indicative of a tight and unaffected barrier (Dejana et al., 2009). As the REC monolayer of the inner retina-blood barrier forms a very tight barrier *in vivo*, our *in vitro* setting very likely reflects the *in vivo* situation more closely (Hofman et al., 2000). Interspecies incompatibility can be ruled out in our experiments, because the used human ANG2 enhances proliferation of iBREC, strongly suggesting that ANG2-specific signaling can be activated with the *human* homologue in this cell line of *bovine* origin. Our observation that ANG2 can enhance the VEGF-A_{165}a-induced decline of the CI (see Fig. 3) also supports this assumption.

That ANG2 enhances the VEGF-A_{165}a-induced impairment of the iBREC barrier is also in accordance with published results from experiments with primary porcine REC (Peters et al., 2007). This effect is most evident at a moderate concentration of VEGF-A_{165}a that is sufficient to induce a slight and transient decline of the CI. Under these conditions ANG2 significantly enhances the VEGF-A_{165}a-caused alteration of the subcellular localization of VEcadherin, further supporting the assumption that this AJ-protein is an important stabilizing component of the REC barrier (Dejana et al., 2009). Although amplification by ANG2 of the VEGF-A-induced changes does not depend on secretion or expression of more VEGF-A by the cells, interplay of both signal transduction pathways contributes to destabilization of the cells' barrier (Rangasamy et al., 2011; Nguyen et al., 2020). However, to prevent weakening of the iBREC barrier by a combination of both growth factors, inhibition of VEGF-A-initiated signaling is sufficient. That dual binding and thereby inactivation of both growth factors with faricimab is not more efficient than VEGF inhibition again confirms VEGF-A's role as the dominant regulator of cellular permeability that cannot be overruled by ANG2-driven signaling. At lower levels of VEGF-A_{165}a, additional inactivation of ANG2 might result in an extra effect, but only in the initial phase of exposure to the growth factors. In addition, the observed difference is very small and likely of minor relevance to the long-term consequences.

Both, deregulated paracellular flow due to re-arranged tight junctions and/or adherens junctions and weaker adhesion of the cells to the extracellular matrix, can contribute to weakening of the REC barrier, but the former process obviously predominates when the barrier impairment is induced by VEGF-A_{165}a together with ANG2 (Atienza et al., 2005; Deissler et al., 2011, 2022; Jäckle et al., 2020). This can be concluded from altered expression and/or subcellular localization of claudin-1 and VEcadherin without integrin α5 being affected.

iBREC internalize both growth factors, and uptake of VEGF-A is not prevented by blocking interaction with its receptors or by inhibition of their tyrosine kinase activities. Therefore, internalization is likely not initiated by formation of complexes of VEGF-A_{165}a and its receptors; at

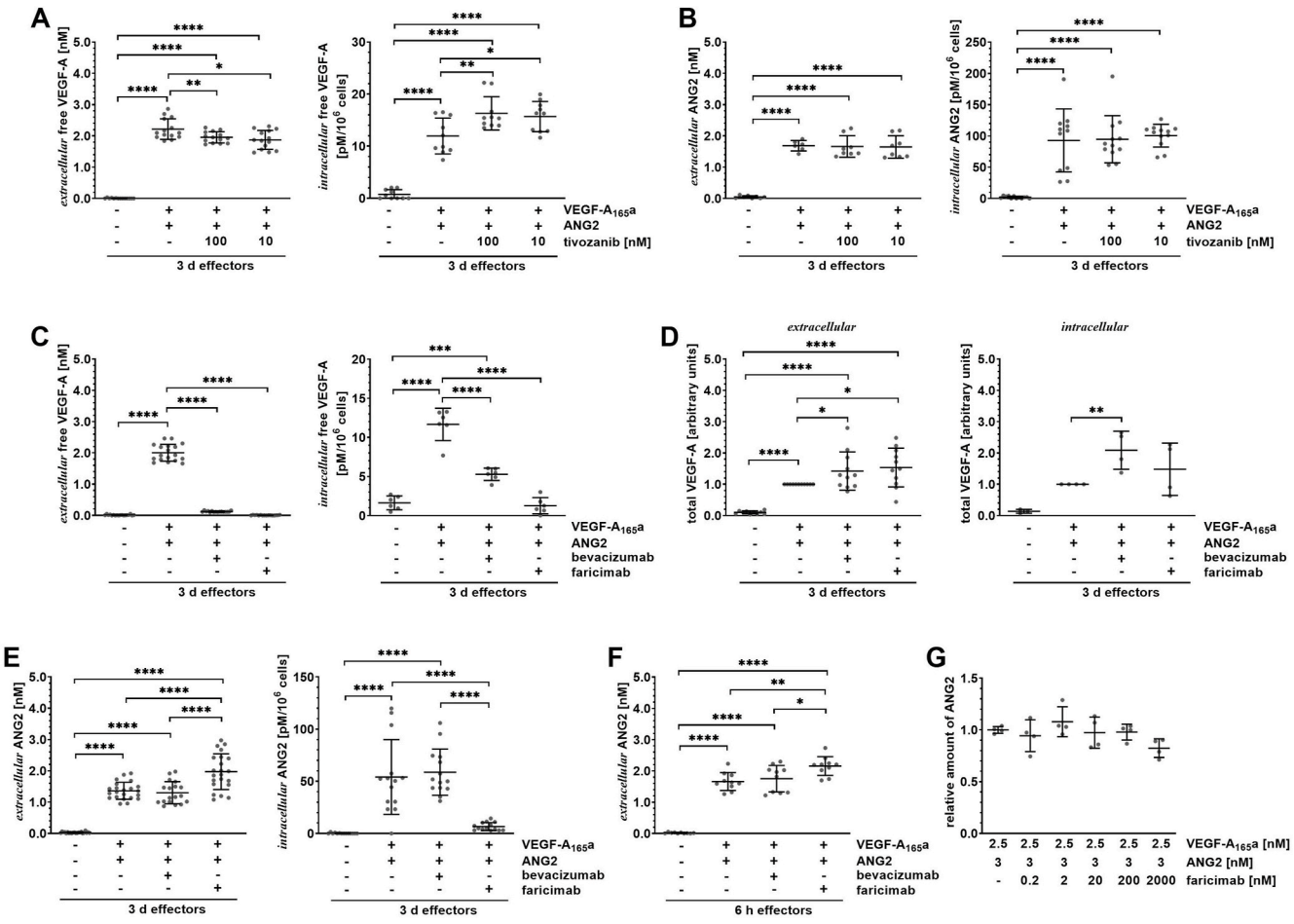

Fig. 8. Faricimab efficiently prevented uptake of ANG2 by iBREC

Confluent iBREC were treated with 2.5 nM VEGF-A_{165}a +3 nM ANG2 with or without tivozanib, 2 μM bevacizumab or 2 μM faricimab for three days before cell culture supernatants were collected or cells were harvested for preparation of cell extracts. Concentrations of (A, C) unbound VEGF-A or (B, E) ANG2 were determined by ELISA or (D) the total amount of VEGF-A was assessed by Western-blotting. (A- C, E) Results of multiple ELISA measurements of several independently prepared cell culture supernatants or cell extracts were pooled and are presented as scatter blots showing means ± standard deviations. Inhibition of the tyrosine kinase activity of VEGF receptor(s) significantly changed levels (A) of extracellular and intracellular VEGF-A but not those of (B) ANG2. (C) Only very low amounts of free VEGF-A, if any, were in cell culture supernatants and cell extracts of iBREC exposed to the growth factor combination and the VEGF antagonists. (D) VEGF-A-specific signals of Western blot analyses were normalized as described in Material and Methods; scatter blots show means and standard deviations of pooled Western blot data; one dot represents the VEGF-A-specific signal from one of multiple independent Western blot analyses. Amounts of VEGF-A in the supernatant were slightly higher when growth factor-treated cells had additionally been exposed to the VEGF antagonists. Cell extracts contained slightly more VEGF-A when growth factor-treated cells had additionally been exposed to bevacizumab. (E) Significantly more ANG2 was measured by ELISA in supernatants of growth factor-treated iBREC which had additionally been exposed to faricimab. In contrast, ANG2 was not detected in cell extracts obtained from similarly treated iBREC. (F) After exposure of confluent iBREC to 2.5 nM VEGF-A_{165}a +3 nM ANG2 with or without 2 μM bevacizumab or 2 μM faricimab for 6 h, cell culture supernatants were collected. Supernatants of growth factor-treated iBREC additionally exposed to faricimab contained significantly more ANG2 as measured by ELISA. (G) The mixture of 2.5 nM VEGF-A_{165}a plus 3 nM ANG2 was incubated with 0.2–2 μM faricimab in a cell-free assay, and presence of ANG2 was assessed by ELISA. Although measured amounts of ANG2 slightly varied in the presence of differing concentrations of faricimab, they were not significantly different from those measured in the absence of the bi-specific antibody. Data were analyzed as described in "2.10 Statistical analyses". *) $p < 0.05$, **) $p < 0.01$, ***) $p < 0.001$, ****) $p < 0.0001$. Only statistically significant differences are shown.

least their tyrosine kinase activity seems not to be necessary (Deissler et al., 2020b). Although uptake of VEGF-A is not prevented by faricimab, free internalized growth factor is not available for initiation of intracellular signaling because it is likely bound to the antagonist; accordingly the barrier is closed (Eichmann and Simons, 2012; Smith et al., 2015). The affinity of bevacizumab to bind to VEGF-A is lower compared to that of faricimab, and indeed low amounts of unbound VEGF-A seem to be present in cell extracts prepared from iBREC exposed to the growth factors and bevacizumab (Presta et al., 1997; Regula et al., 2016). That the detection antibodies of the ELISA used not only bind to free VEGF-A, but also – although with a much lower affinity – to the VEGF-A/bevacizumab complex is a reasonable explanation for this observation (Sumner et al., 2019). The ELISA detection antibodies might also replace bevacizumab in the VEGF-A/bevacizumab complex, resulting in detection of VEGF-A by ELISA without ruling out full inactivation of intra- and extracellular VEGF-A in tight complexes with bevacizumab *in vivo*. Anyway, measured amounts of unbound VEGF-A are too low to initiate or maintain a dysfunction of the iBREC barrier and, accordingly, the barrier remains tightly closed (Deissler et al., 2011, 2022). Similar to VEGF-A, ANG2 is internalized by iBREC to be subsequently degraded, as concluded from continuously decreasing extra- and intracellular levels. Interestingly, uptake of ANG2 is strongly prevented by faricimab which interferes with binding of the growth factor to its receptor Tie2, suggesting that internalization of ANG2 – at least partly – depends on interaction with this receptor (Regula et al., 2016).

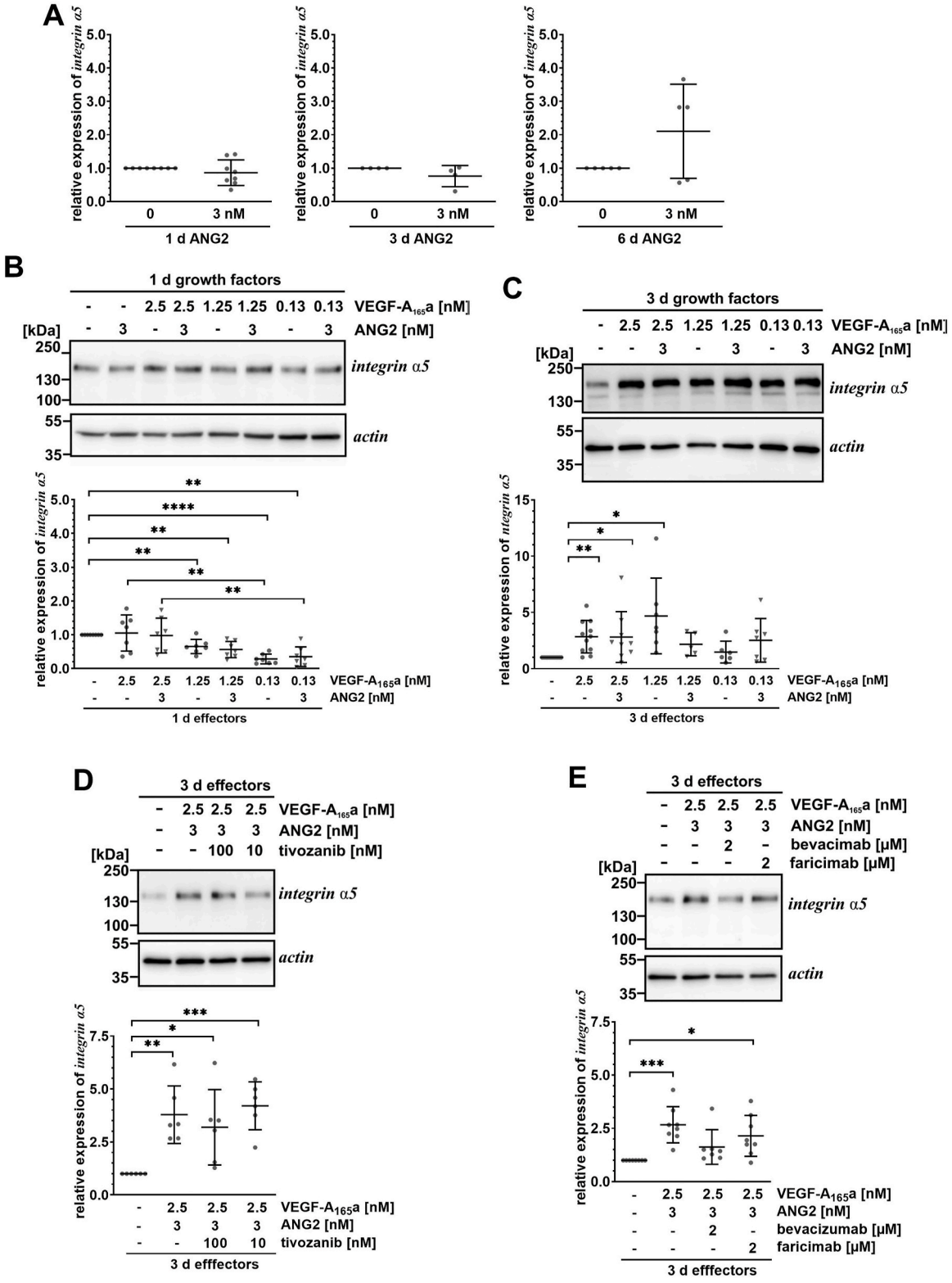

Fig. 9. VEGF-A$_{165}$a, but not ANG2 modulated expression of integrin α5

After establishing a confluent monolayer, iBREC were exposed to (A) ANG2, (B, C) 0.13 nM–2.5 nM VEGF-A$_{165}$a with or without 3 nM ANG2, or (D, E) to VEGF-A$_{165}$a + ANG2 in the absence or presence of tivozanib, bevacizumab or faricimab, respectively, before cells were harvested for preparation of cell extracts at indicated time points. Signals of multiple Western blot analyses specific for integrin α5 were normalized and pooled, and are shown as scatter blots with means and standard deviations as described above. (A) Extended incubation of iBREC with ANG2 did not alter expression of integrin α5. (B) Only ≤1.25 nM VEGF-A$_{165}$a significantly lowered protein amounts of integrin α5, the effect was not modulated by ANG2. (C) Treatment with ≥1.25 nM VEGF-A$_{165}$a for three days led to significantly more integrin α5 also not modulated by ANG2 (D) Tivozanib, (E) bevacizumab or faricimab did not prevent higher amounts of integrin α5 induced by growth factor-treatment. Data were analyzed as described in "2.10 Statistical analyses". *). $p < 0.05$, **) $p < 0.01$, ***) $p < 0.001$, ****) $p < 0.0001$, indicating only statistically significant differences.

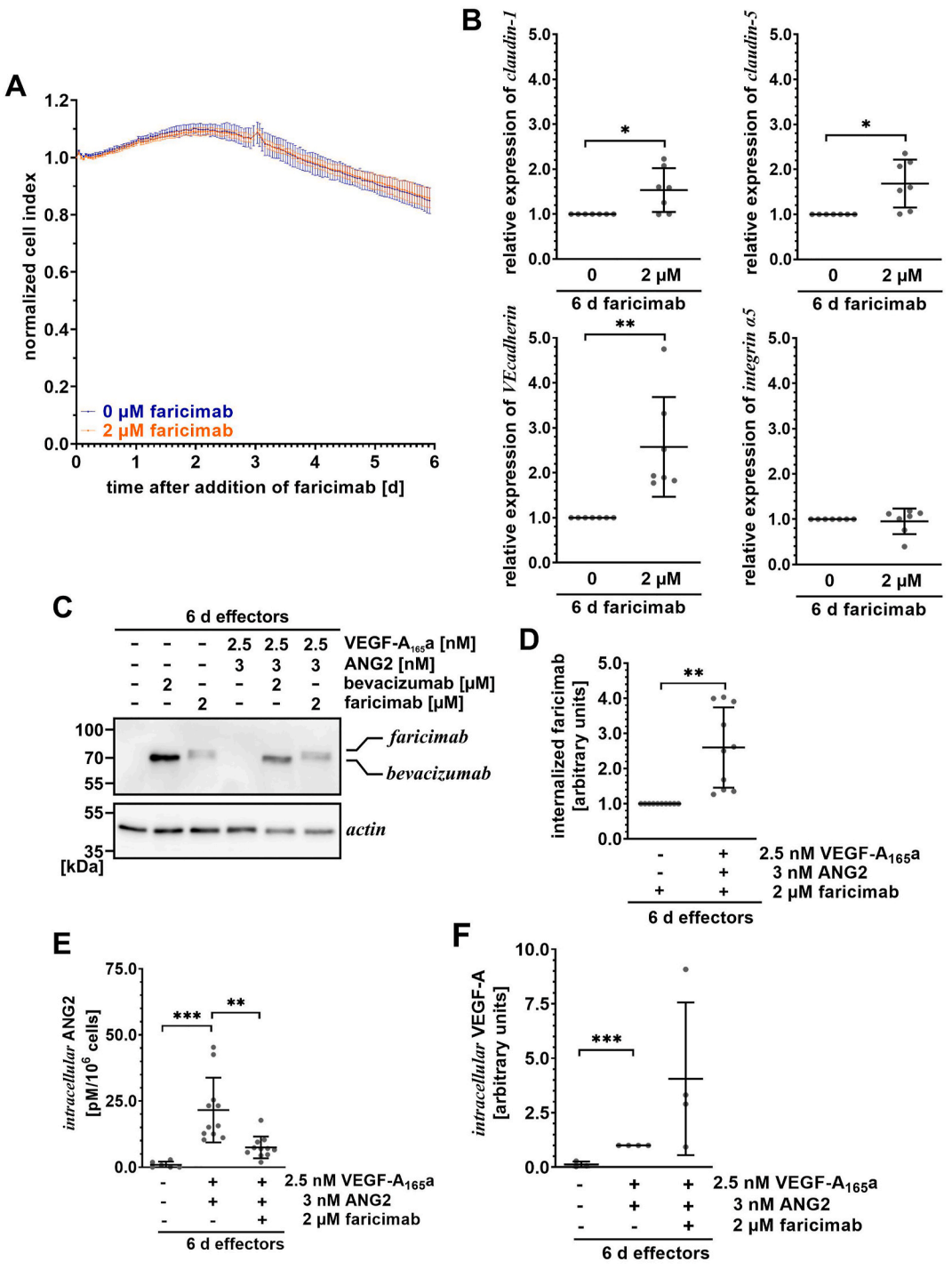

Fig. 10. Prolonged exposure of iBREC to faricimab stabilized their barrier

iBREC were treated with faricimab in the absence or presence of VEGF-A_{165}a + ANG2 for six days, and (A) the CI was followed continuously or (B–F) cell extracts were prepared. (A) CI values obtained from at least six wells per condition and time point were normalized as described above. Faricimab did not change the CI compared to unchallenged cells. (B, D, F) Specific signals of Western blot analyses were normalized and pooled, and are shown as scatter blots with means and standard deviations as described above. (B) Significantly more claudin-1, claudin-5 and VEcadherin were measured after extended treatment of iBREC with faricimab. (C, D) Faricimab and bevacizumab were present in cell extracts obtained from iBREC treated with the VEGF antagonists in the absence or presence of VEGF-A_{165}a + ANG2; amounts of internalized faricimab were significantly higher in growth factor-treated cells. (E) Results of multiple ELISA measurements of several independently prepared cell extracts were pooled and are presented as scatter blots showing means ± standard deviations. Levels of internalized ANG2 were significantly lower in growth factor-treated cells additionally exposed to faricimab. (F) Internalized amounts of VEGF-A were not changed by additional exposure of the cells to faricimab. Data were analyzed as described in "2.10 Statistical analyses". *) $p < 0.05$, **) $p < 0.01$, ***) $p < 0.001$. Only statistically significant differences are indicated.

Long-term exposure of iBREC to faricimab does not affect the cells' viability, confirming our previous observation that inhibition of VEGF-A-driven signaling is not harmful to retinal endothelial cells per se (Deissler et al., 2020a). Similar to bevacizumab, faricimab is also taken up by iBREC (Deissler et al., 2016). Whereas internalization of bevacizumab is mediated by the neonatal Fc receptor/transporter (FcRn), uptake of faricimab cannot depend on this route, because due to its modified Fc terminus the bi-specific antibody is not able to bind to the FcRn (Junghans and Anderson, 1996; Deissler et al., 2012, 2016; Regula et al., 2016). Interestingly, more faricimab is internalized by the cells in the presence of both target proteins. As the amounts of measured intracellular ANG2 are then only very low, most of the internalized faricimab is either unladen or bound only to VEGF-A, inviting the speculation that this complex is more stable. However, the observed stable barrier function suggests that possible accumulation of the VEGF-A/faricimab complex is not harmful to iBREC.

Taken together, the results of our *in vitro* study suggest that ANG2 modulates but does not overrule the dominant impairing effects of VEGF-A_{165}a on the barrier formed by REC. However, other processes may also play important roles in the more complex *in vivo* situation. REC are *in vivo* in contact with retinal pericytes (RP), and interaction with these cells is of physiological relevance and often disrupted in diabetes (Kovacs-Oller et al., 2020). ANG2 might be involved in such pathophysiological processes as it was identified as a potential cause of RP loss in early stages of diabetic retinopathy (Hammes et al., 2004). This might be due to accumulation of ANG2 in the retina as a consequence of its secretion by REC under hyperglycemia or induced by VEGF-A_{165}a as observed *in vitro* (Rangasamy et al., 2011; Eyre et al., 2020; McCann et al., 2023). ANG2 can also stimulate proliferation of REC, a process likely involved in retinal neovascularization. Although blocking VEGF-A-initiated signaling by intravitreal injection of VEGF-binding proteins is in general a successful therapeutic approach to treat macular edema, a subgroup of patients does not respond sufficiently for reasons yet unknown (Ferrara et al., 2006; Presta et al., 1997; Mitchell et al., 2011; Wells et al., 2015; Busch et al., 2018; Maggio et al., 2018). Particularly in these cases, additional targeting of ANG2 with the bi-specific antibody faricimab might be beneficial through prevention of retinal neovascularization or RP loss rather than by additional stabilization of the REC barrier.

5. Conclusion

In the regulation of REC permeability, VEGF-driven signaling overrules effects of ANG2, although ANG2 transiently enhances the VEGF-A-induced impairment of the REC barrier. Such barrier disturbance can be prevented with similar efficiencies by sole inhibition of VEGF-A-driven signaling or dual inactivation of both growth factors with faricimab.

Funding statement

For part of this research, Heidrun L. Deissler received funding from Giessener Lichtblicke e.V., Giessen, Germany. The funding source did not have any influence on study design, data analyses and interpretation, writing of the manuscript and decision on publishing. Open Access funding was enabled and organized by Projekt DEAL.

Financial disclosure

Heidrun L. Deissler is receiving research funding from ROCHE Pharma AG. Lyubomyr Lytvynchuk has no conflicts of interest to declare. Matus Rehak is a consultant for Allergan, Alimera Sciences Ophthalmologie GmbH, Bayer AG and Novartis Pharma GmbH, and received speaker honoraria from Allergan, Alimera Sciences Ophthalmologie GmbH, Bayer AG, Novartis Pharma GmbH and Zeiss.

CRediT authorship contribution statement

Heidrun L. Deissler: Writing – review & editing, Writing – original draft, Validation, Supervision, Methodology, Investigation, Formal analysis, Conceptualization. **Matus Rehak:** Writing – review & editing, Validation, Supervision, Formal analysis. **Lyubomyr Lytvynchuk:** Writing – review & editing, Validation, Supervision.

Data availability

Data will be made available on request.

Acknowledgements and statements

The authors thank Stefanie Woelfel for expert technical assistance. They are particularly grateful to Professor Helmut Deissler, HD/U Giessen, Germany, for his steady advice and for supporting the preparation of the manuscript.

No ethical conflicts have to be disclosed by the authors.

This article does not contain any results of studies with human participants or animals.

Appendix A. Supplementary data

Supplementary data to this article can be found online at https://doi.org/10.1016/j.exer.2024.110062.

References

Aiello, L.P., Avery, R.L., Arrigg, P.G., Keyt, B.A., Jampel, H.D., Shah, S.T., Pasquale, L.R., Thieme, H., Iwamoto, M.A., Park, J.E., Nguyen, H.V., Aiello, L.M., Ferrara, N., King, G.L., 1994. Vascular endothelial growth factor in ocular fluid of patients with diabetic retinopathy and other retinal disorders. N. Engl. J. Med. 331, 1480–1487. https://doi.org/10.1056/NEJM199412013312203.

Antonetti, D.A., Barber, A.J., Hollinger, L.A., Wolpert, E.B., Gardner, T.W., 1999. Vascular endothelial growth factor induces rapid phosphorylation of tight junction proteins occludin and zonula occludens 1. J. Biol. Chem. 274, 23463–23467. https://doi.org/10.1074/jbc.274.33.23463.

Atienza, J.M., Zhu, J., Wang, X., Xu, X., Abassi, Y., 2005. Dynamic monitoring of cell adhesion and spreading on microelectronic sensor arrays. J. Biomol. Screen 10, 795–805. https://doi.org/10.1177/1087057105279635.

Barton, W.A., Tzvetkova-Robev, D., Miranda, E.P., Kolev, M.V., Rajashankar, K.R., Himanen, J.P., Nikolov, D.B., 2006. Crystal structures of the Tie2 receptor ectodomain and the angiopoietin-2-Tie2 complex. Nat. Struct. Mol. Biol. 13, 524–532. https://doi.org/10.1038/nsmb1101.

Bates, D., Mavrou, A., Qiu, Y., Carter, J.G., Hamdollah-Zadeh, M., Barratt, S., Gammons, M.V., Millar, A.B., Salmon, A.H.J., Oltean, S., Harper, S.J., 2018. Detection of VEGF-A(xxx)b isoforms in human tissues. PLoS One 8, e68399. https://doi.org/10.1371/journal.pone.0068399 eCollection 2016.

Boulton, M., Gregor, Z., McLeod, D., Charteris, D., Jarvis-Evans, J., Moriatry, P., Khaliq, A., Foreman, D., Allamby, D., Bardsley, B., 1997. Intravitreal growth factors in proliferative diabetic retinopathy: correlation with neovascular activity and glycaemic management. Br. J. Ophthalmol. 81, 228–233. https://doi.org/10.1136/bjo.81.3.228.

Busch, C., Zur, D., Fraser-Bell, S., Laíns, I., Santos, A.R., Lupidi, M., Cagini, C., Gabrielle, P.H., Couturier, A., Mané-Tauty, V., Giancipoli, E., Ricci, G.D., Cebeci, Z., Rodríguez-Valdés, P.J., Chaikitmongkol, V., Amphornphruet, A., Hindi, I., Agrawal, K., Chhablani, J., Loewenstein, A., Iglicki, M., Rehak, M., International Retina Group, 2018. Shall we stay, or shall we switch? Continued anti-VEGF therapy versus early switch to dexamethasone implant in refractory diabetic macular edema. Acta Diabetol. 55, 789–796. https://doi.org/10.1007/s00592-018-1151-x.

Busch, C., Rehak, M., Hollborn, M., Wiedemann, P., Lang, G.K., Lang, G.E., Wolf, A., Deissler, H.L., 2021. Type of culture medium determines properties of cultivated retinal endothelial cells: induction of substantial phenotypic conversion by standard DMEM. Heliyon 7, e06037. https://doi.org/10.1016/j.heliyon.2021.e06037.

Campochiaro, P.A., 2000. Retinal and choroidal neovascularization. J. Cell. Physiol. 184, 301–310.

Campochiaro, P.A., 2013. Ocular neovascularization. J. Mol. Med. 91, 311–321.

Castellon, R., Hamdi, H.K., Sacerio, I., Aoki, A.M., Kenney, M.C., Ljubimov, A.V., 2002. Effects of angiogenic growth factor combinations on retinal endothelial cells. Exp. Eye Res. 74, 523–535. https://doi.org/10.1006/exer.2001.1161.

Deissler, H., Deissler, H., Lang, G.K., Lang, G.E., 2005. Generation and characterization of iBREC: novel hTERT-immortalized bovine retinal endothelial cells. Int. J. Mol. Med. 15, 65–70. https://doi.org/10.3892/ijmm.16.1.65.

Deissler, H., Deissler, H., Lang, G.E., 2011. Inhibition of VEGF is sufficient to completely restore barrier malfunction induced by growth factors in microvascular retinal

endothelial cells. Br. J. Ophthalmol. 95, 1151–1156. https://doi.org/10.1136/bjo.2010.192229.
Deissler, H., Deissler, H., Lang, G.E., 2012. Actions of bevacizumab and ranibizumab on microvascular retinal endothelial cells: similarities and differences. Br. J. Ophthalmol. 96, 1023–1028. https://doi.org/10.1136/bjophthalmol-2012-301677.
Deissler, H.L., Deissler, H., Lang, G.K., Lang, G.E., 2013. Ranibizumab efficiently blocks migration but not proliferation induced by growth factor combinations including VEGF in retinal endothelial cells. Graefes Arch. Clin. Exp. Ophthalmol. 251, 2345–2353. https://doi.org/10.1007/s00417-013-2393-5.
Deissler, H.L., Lang, G.K., Lang, G.E., 2016. Internalization of bevacizumab by retinal endothelial cells and its intracellular fate: evidence for an involvement of the neonatal Fc receptor. Exp. Eye Res. 143, 49–59. https://doi.org/10.1016/j.exer.2015.10.007.
Deissler, H.L., Lang, G.K., Lang, G.E., 2017. Inhibition of single routes of intracellular signaling is not sufficient to neutralize the biphasic disturbance of a retinal endothelial cell barrier induced by VEGF-A_{165}. Cell. Physiol. Biochem. 42, 1493–1513. https://doi.org/10.1159/000479213.
Deissler, H.L., Stutzer, J.-N., Lang, G.K., Grisanti, S., Lang, G.E., Ranjbar, M., 2020a. VEGF receptor 2 inhibitor nintedanib completely reverts VEGF-A_{165}-induced disturbances of barriers formed by retinal endothelial cells or long-term cultivated ARPE-19 cells. Exp. Eye Res. 194, 108004 https://doi.org/10.1016/j.exer.2020.108004.
Deissler, H.L., Sommer, K., Lang, G.K., Lang, G.E., 2020b. Transport and fate of aflibercept in VEGF-A_{165}-challenged retinal endothelial cells. Exp. Eye Res. 198, 108156 https://doi.org/10.1016/j.exer.2020.108156.
Deissler, H.L., Rehak, M., Busch, C., Wolf, A., 2022. Blocking of VEGF-A is not sufficient to completely revert its long-term effects on the barrier formed by retinal endothelial cells. Exp. Eye Res. 216, 108945 https://doi.org/10.1016/j.exer.2022.108945.
Dejana, E., Tournier-Lasserve, E., Weinstein, B.M., 2009. The control of vascular integrity by endothelial cell junctions: molecular basis and pathological implications. Dev. Cell 16, 209–221. https://doi.org/10.1016/j.devcel.2009.01.004.
Eichmann, A., Simons, M., 2012. VEGF signaling inside vascular endothelial cells and beyond. Curr. Opin. Cell Biol. 24, 188–193. https://doi.org/10.1016/j.ceb.2012.02.002.
Eyre, J.J., Williams, R.L., Levis, H.J., 2020. A human retinal microvascular endothelial-pericyte co-culture model to study diabetic retinopathy in vitro. Exp. Eye Res. 201, 108293 https://doi.org/10.1016/j.exer.2020.108293.
Ferrara, N., Damico, L., Shams, N., Lowman, H., Kim, R., 2006. Development of ranibizumab, an anti-vascular endothelial growth factor antigen binding fragment, as therapy for neovascular age-related macular degeneration. Retina 26, 859–870. https://doi.org/10.1097/01.iae.0000242842.14624.e7.
Fiedler, U., Scharpfenecker, M., Koidl, S., Hegen, A., Grunow, V., Schmidt, J.M., Kriz, W., Thurston, G., Augustin, H.G., 2004. The tie-2 ligand angiopoietin-2 is stored in and rapidly released upon stimulation from endothelial cell Weibel-Palade bodies. Blood 103, 4150–4156. https://doi.org/10.1182/blood-2003-10-3685.
Hammes, H.P., Lin, J., Wagner, P., Feng, Y., Vom Hagen, F., Krzizok, T., Renner, O., Breier, G., Brownlee, M., Deutsch, U., 2004. Angiopoietin-2 causes pericyte dropout in the normal retina: evidence for involvement in diabetic retinopathy. Diabetes 53, 1104–1110. https://doi.org/10.2337/diabetes.53.4.1104.
Hofman, P., Blaauwgeers, H.G., Tolentino, M.J., Adamis, A.P., Nunes Cardozo, B.J., Vrensen, G.F., Schlingemann, R.O., 2000. VEGF-A induced hyperpermeability of blood-retinal barrier endothelium in vivo is predominantly associated with pinocytotic vesicular transport and not with formation of fenestrations. Curr. Eye Res. 21, 637–645.
Jäckle, A., Ziemssen, F., Kuhn, E.M., Kampmeier, J., Lang, G.K., Lang, G.E., Deissler, H., Deissler, H.L., 2020. Sitagliptin and the blood-retina barrier: effects on retinal endothelial cells manifested only after prolonged exposure. J. Diabetes Res. 2020, 2450781. https://doi.org/10.1155/2020/2450781.
Junghans, R.P., Anderson, C.L., 1996. The protection receptor for IgG catabolism is the β_2-microglobulin-containing neonatal intestinal transport receptor. Proc. Natl. Acad. Sci. USA 93, 5512–5516. https://doi.org/10.1073/pnas.93.11.5512.
Kanchanawong, P., Calderwood, D.A., 2023. Organization, dynamics and mechanoregulation of integrin-mediated cell–ECM adhesions. Nat. Rev. Mol. Cell Biol. 24, 142–161. https://doi.org/10.1038/s41580-022-00531-5.
Khan, M., Aziz, A.A., Shafi, N.A., Abbas, T., Khanani, A.M., 2020. Targeting Angiopoietin in retinal vascular diseases: a literature review and summary of clinical trials involving faricimab. Cells 9, 1869. https://doi.org/10.3390/cells9081869.
Kinnunen, K., Puustjärvi, T., Teräsvirta, M., Nurmenniemi, P., Heikura, T., Laidinen, S., Paavonen, T., Uusitalo, H., Ylä-Herttuala, S., 2009. Differences in retinal neovascular tissue and vitreous humour in patients with type 1 and type 2 diabetes. Br. J. Opthalmol. 93, 1109–1115. https://doi.org/10.1136/bjo.2008.148841.
Klaassen, I., deVries, E.W., Vogels, I.M.C., van Kampen, A.H.C., Bosscha, M.I., Steel, D.H.W., Van Noorden, C.J.F., Lesnik-Oberstein, S.Y., Schlingemann, R.O., 2017. Identification of proteins associated with clinical and pathological features of proliferative diabetic retinopathy in vitreous and fibrovascular membrane. PLoS One 12, e0187304. https://doi.org/10.1371/journal.pone.0187304 eCollection 2017.
Klaassen, I., Avery, P., Schlingemann, R.O., Steel, D.H.W., 2022. Vitreous protein networks around ANG2 and VEGF in proliferative diabetic retinopathy and the different effects of aflibercept versus bevacizumab pre-treatment. Sci. Rep. 12, 21062 https://doi.org/10.1038/s41598-022-25216-z.
Kluger, M.S., Clark, P.R., Tellides, G., Gerke, V., Pober, J.S., 2014. Claudin-5 controls intercellular barriers of human dermal microvascular but not human umbilical vein endothelial cells. Arterioscler. Thromb. Vasc. Biol. 33, 489–500. https://doi.org/10.1161/ATVBAHA.112.300893.
Kovacs-Oller, T., Ivanova, E., Bianchimano, P., Sagdullaev, B.T., 2020. The pericyte connectome: spatial precision of neurovascular coupling is driven by selective connectivity maps of pericytes and endothelial cells and is disrupted in diabetes. Cell Discov 6, 39. https://doi.org/10.1038/s41421-020-0180-0.
Maggio, E., Sartore, M., Attanasio, M., Maraone, G., Guerriero, M., Polito, A., Pertile, G., 2018. Anti-vascular endothelial growth factor treatment for diabetic macular edema in a real-world clinical setting. Am. J. Ophthalmol. 195, 209–222. https://doi.org/10.1016/j.ajo.2018.08.004.
Maisonpierre, P.C., Suri, C., Jones, P.F., Bartunkova, S., Wiegand, S.J., Radziejewski, C., Compton, D., McClain, J., Aldrich, T.H., Papadopoulos, N., Daly, T.J., Davis, S., Sato, T.N., Yancopoulos, G.D., 1997. Angiopoietin-2, a natural antagonist for Tie2 that disrupts in vivo angiogenesis. Science 277, 55–60. https://doi.org/10.1126/science.277.5322.55.
McCann, M., Li, Y., Baccouche, B. Kazlauskas A., 2023. VEGF induces expression of genes that either promote or limit relaxation of the retinal endothelial barrier. Int. J. Mol. Sci. 24, 6402. https://doi.org/10.3390/ijms24076402.
Mitchell, P., Bandello, F., Schmidt-Erfurth, U., Lang, G.E., Massin, P., Schlingemann, R. O., Sutter, F., Simader, C., Burian, G., Gerstner, O., Weichselberger, A., Restore, study group, 2011. The RESTORE study: ranibizumab monotherapy or combined with laser versus laser monotherapy for diabetic macular edema. Ophthalmology 118, 615–625. https://doi.org/10.1016/j.ophtha.2011.01.031.
Muellerleile, L.M., Buxbaum, B., Nell, B., Fux, D.A., 2019. In-vitro binding analysis of anti-human vascular endothelial growth factor antibodies bevacizumab and aflibercept with canine, feline, and equine vascular endothelial growth factor. Res. Vet. Sci. 124, 233–238. https://doi.org/10.1016/j.rvsc.2019.03.018.
Nakamura, K., Taguchi, E., Miura, T., et al., 2006. KRN951, a highly potent inhibitor of vascular endothelial growth factor receptor tyrosine kinases, has antitumor activities and affects functional vascular properties. Cancer Res. 66, 9134–9142. https://doi.org/10.1158/0008-5472.CAN-05-4290.
Nguyen, Q.D., Heier, J.S., Do, D.V., Mirando, A.C., Pandey, N.B., Sheng, H., Heah, T., 2020. The Tie2 signaling pathway in retinal vascular diseases: a novel therapeutic target in the eye. Int. J. Retin. Vitr. 6, 48. https://doi.org/10.1186/s40942-020-00250-z.
Pergolizzi, M., Bizzozero, L., Riccitelli, E., Pascal, D., Samarelli, A.V., Bussolino, F., Arese, M., 2018. Modulation of Angiopoietin 2 release from endothelial cells and angiogenesis by the synaptic protein Neuroligin 2. Biochem. Biophys. Res. Commun. 501, 165–171. https://doi.org/10.1016/j.bbrc.2018.04.204.
Peters, S., Cree, I.A., Alexander, R., Turowski, P., Ockrim, Z., Patel, J., Boyd, S.R., Joussen, A.M., Ziemssen, F., Hykin, P.G., Moss, S.E., 2007. Angiopoietin modulation of vascular endothelial growth factor: effects on retinal endothelial cell permeability. Cytokine 40, 144–150. https://doi.org/10.1016/j.cyto.2007.09.001.
Presta, L.G., Chen, H., O'Connor, S.J., Chisholm, V., Meng, Y.G., Krummen, L., Winkler, M., Ferrara, N., 1997. Humanization of an anti-vascular endothelial growth factor monoclonal antibody for the therapy of solid tumors and other disorders. Cancer Res. 57, 4593–4599.
Qaum, T., Xu, Q., Joussen, A.M., Clemens, M.W., Qin, W., Miyamoto, K., Hassessian, H., Wiegand, S.J., Rudge, J., Yancopoulos, G.D., Adamis, A.P., 2001. VEGF-initiated blood-retinal barrier breakdown in early diabetes. Invest. Ophthalmol. Vis. Sci. 42, 2408–2413.
Rangasamy, S., Srinivasan, R., Maestas, J., McGuire, P.G., Das, A., 2011. A potential role for angiopoietin 2 in the regulation of the blood–retinal barrier in diabetic retinopathy. Invest. Ophthalmol. Vis. Sci. 52, 3784–3791. https://doi.org/10.1167/iovs.10-6386.
Regula, J.T., Lundh von Leithner, P., Foxton, R., Barathi, V.A., Cheung, C.M., Bo, Tun S. B., Wey, Y.S., Iwata, D., Dostalek, M., Moelleken, J., Stubenrauch, K.G., Nogoceke, E., Widmer, G., Strassburger, P., Koss, M.J., Klein, C., Shima, D.T., Hartmann, G., 2016. Targeting key angiogenic pathways with a bispecific CrossMAb optimized for neovascular eye diseases. EMBO Mol. Med. 8, 1265–1288. https://doi.org/10.15252/emmm.201505889. Correctionsin: EMBO Mol. Med. 2017 9, 985. EMBO Mol. Med. 2019 11, e10666.
Saharinen, P., Bry, M., Alitalo, K., 2010. How do angiopoietins Tie in with vascular endothelial growth factors? Curr. Opin. Hematol. 17, 198–205. https://doi.org/10.1097/MOH.0b013e3283386673.
Smith, G.A., Fearnley, G.W., Tomlinson, D.C., Harrison, M.A., Ponnambalam, S., 2015. The cellular response to vascular endothelial growth factors requires co-ordinated signal transduction, trafficking and proteolysis. Biosci. Rep. 35, e00253 https://doi.org/10.1042/BSR20150171.
Suarez, S., McCollum, G.W., Bretz, C.A., Yang, R., Capozzi, M.E., Penn, J.S., 2014. Modulation of VEGF-induced retinal vascular permeability by peroxisome proliferator-activated receptor-β/δ. Invest. Ophthalmol. Vis. Sci. 55, 8232–8240. https://doi.org/10.1167/iovs.14-14217.
Sumner, G., Georgaros, C., Rafique, A., DiCioccio, T., Martin, J., Papadopoulos, N., Daly, T., Torri, A., 2019. Anti-VEGF drug interference with VEGF quantitation in the R&D systems human quantikine VEGF ELISA kit. Bioanalysis 11, 381–392. https://doi.org/10.4155/bio-2018-0096.
Sun, M., Fu, H., Cheng, H., Cao, Q., Zhao, Y., Mou, X., Zhang, X., Liu, X., Ke, Y., 2012. A dynamic real-time method for monitoring epithelial barrier function in vitro. Anal. Biochem. 425, 96–103. https://doi.org/10.1016/j.ab.2012.03.010.
Walz, J.M., Boehringer, D., Deissler, H.L., Faerber, L., Goepfer, J., Heiduschka, P., Kleeberger, S.M., Klettner, A., Krohne, T.U., Schneiderhan-Marra, N., Ziemssen, F., Stahl, A., 2016. Pre-analytical parameters affecting vascular endothelial growth factor measurement in plasma: identifying confounders. PLoS One 11, e0145375. https://doi.org/10.1371/journal.pone.0145375 eCollection 2016.
Watanabe, D., Suzuma, K., Suzuma, I., Ohashi, H., Ojima, T., Kurimoto, M., Murakami, T., Kimura, T., Takagi, H., 2005. Vitreous levels of angiopoietin 2 and vascular endothelial growth factor in patients with proliferative diabetic retinopathy. Am. J. Ophthalmol. 139, 476–481. https://doi.org/10.1016/j.ajo.2004.10.004.

Wells, J.A., Glassman, A.R., Ayala, A.R., Jampol, L.M., Aiello, L.P., Antoszyk, A.N., Arnold-Bush, B., Baker, C.W., Bressler, N.M., Browning, D.J., Elman, M.J., Ferris, F. L., Friedman, S.M., Melia, M., Pieramici, D.J., Sun, J.K., Beck, R.W., Diabetic Retinopathy Clinical Research Network., 2015. Aflibercept, bevacizumab, or ranibizumab for diabetic macular edema. N. Engl. J. Med. 372, 1193–1203. https://doi.org/10.1056/NEJMoa1414264.

Wisniewska-Kruk, J., Hoeben, K.A., Vogels, I.M., Gaillard, P.J., Van Noorden, C.J., Schlingemann, R.O., Klaassen, I., 2012. A novel co-culture model of the blood-retinal barrier based on primary retinal endothelial cells, pericytes and astrocytes. Exp. Eye Res. 96, 181–190. https://doi.org/10.1016/j.exer.2011.12.003.

Wisniewska-Kruk, J., van der Wijk, A.E., van Veen, H.A., Gorgels, T.G., Vogels, I.M., Versteeg, D., Van Noorden, C.J., Schlingemann, R.O., Klaassen, I., 2016. Plasmalemma vesicle-associated protein has a key role in blood-retinal barrier loss. Am. J. Pathol. 186, 1044–1054. https://doi.org/10.1016/j.ajpath.2015.11.019.

Wong, T.Y., Haskova, Z., Asik, K., Baumal, C.R., Csaky, K.G., Eter, N., Ives, J.A., Jaffe, G. J., Korobelnik, J.F., Lin, H., Murata, T., Ruamviboonsuk, P., Schlottmann, P.G., Seres, A.I., Silverman, D., Sun, X., Tang, Y., Wells, J.A., Yoon, Y.H., Wykoff, C.C., YOSEMITE and RHINE investigators., 2023. Faricimab treat-and-extend for diabetic macular edema: 2-year results from the randomized phase 3 YOSEMITE and RHINE trials. Ophthalmology 27. https://doi.org/10.1016/j.ophtha.2023.12.026. S0161-6420(23)00933-8.